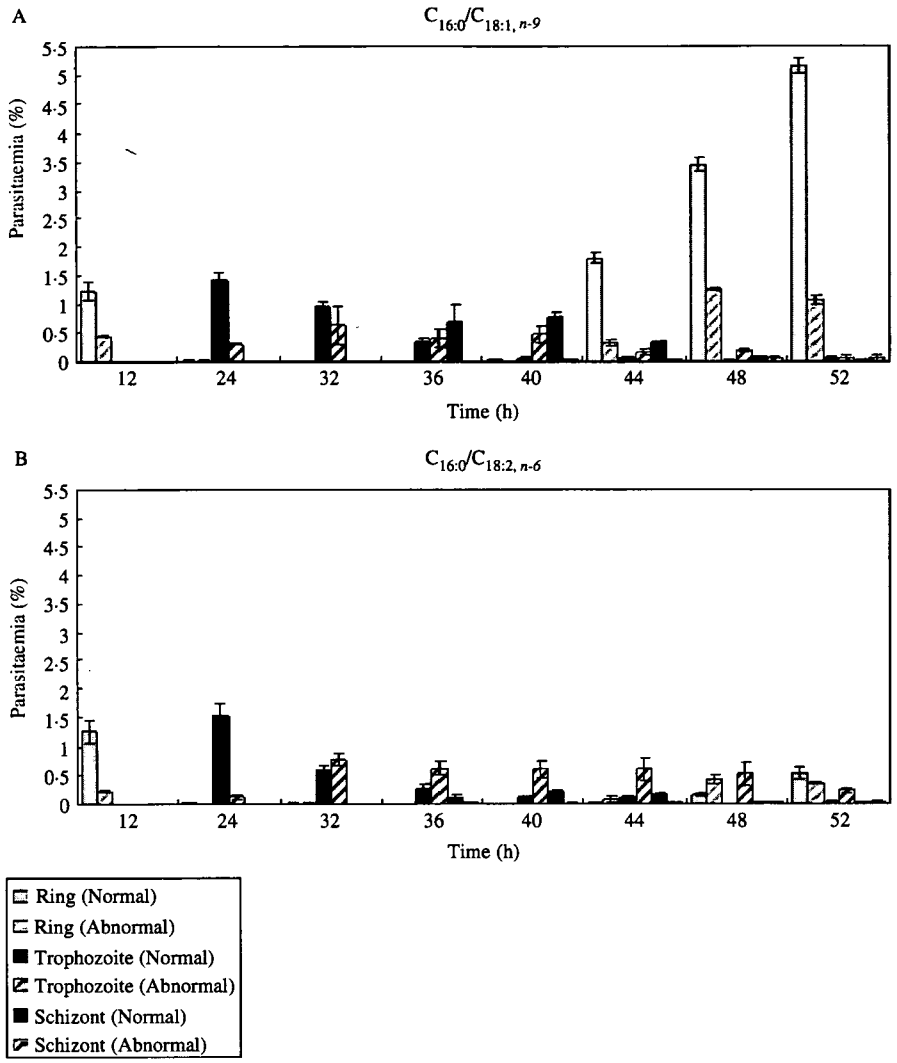

Fig. 5. Distribution of each stage during the course of intraerythrocytic development. Parasitaemia was determined at different stages in cultures grown in serum-free medium supplemented with reconstituted lipid-associated BSA containing a combination of fatty acids. (A) $C_{16:0}/C_{18:1,n-9}$. (B) $C_{16:0}/C_{18:2,n-6}$. Parasites of normal appearance and those of abnormal appearance were counted separately. Starting parasitaemia was set at 1·57%. Final concentrations of fatty acids used were $C_{16:0}/C_{18:1,n-9}$, 30 μM/30 μM; $C_{16:0}/C_{18:2,n-6}$, 30 μM/30 μM. Error bar indicates the difference from the average.

medium containing $C_{16:0}/C_{18:2,n-6}$, as in parasites grown in medium containing $C_{16:0}/C_{18:1,n-9}$, parasites of normal appearance proceeded to trophozoite and schizont stages, and newly formed rings appeared from 44 h (Fig. 5B). In addition, the numbers of newly formed rings were much lower than in cultures grown in medium containing $C_{16:0}/C_{18:1,n-9}$. These results imply that, despite supporting the intraerythrocytic development of *P. falciparum*, the population of parasites that entered the next erythrocytic cycle differed between $C_{18:1,n-9}$ combined with $C_{16:0}$ and $C_{18:2,n-6}$ combined with $C_{16:0}$.

With respect to parasites of abnormal appearance, in medium containing $C_{16:0}/C_{18:1,n-9}$, only a minor population of parasitized erythrocytes (in <40% of total parasitized erythrocytes) were abnormal. However, in medium containing $C_{16:0}/C_{18:2,n-6}$, from 32 h on, large numbers of abnormal trophozoites were observed (in >50% of total parasitized erythrocytes), and these were predominant at 44 h.

Differences in the effects of unsaturated fatty acid species on stage progression became more evident when we compared stage distribution by percentage (Fig. 6). We focused only on parasites of normal appearance. From 36 h onwards, the distribution of stages in medium containing $C_{16:0}/C_{18:1,n-9}$ is statistically different from that in medium containing $C_{16:0}/C_{18:2,n-6}$ (Cochran-Mantel-Haenszel P-values: 0·56 at 24 h; 0·0001 at 36 h; <0·0001 at 40 h; <0·0001 at 44 h). In fact, synchronicity was well maintained until 24 h, at the trophozoite stage, in media containing $C_{16:0}/C_{18:1,n-9}$ or $C_{16:0}/C_{18:2,n-6}$.

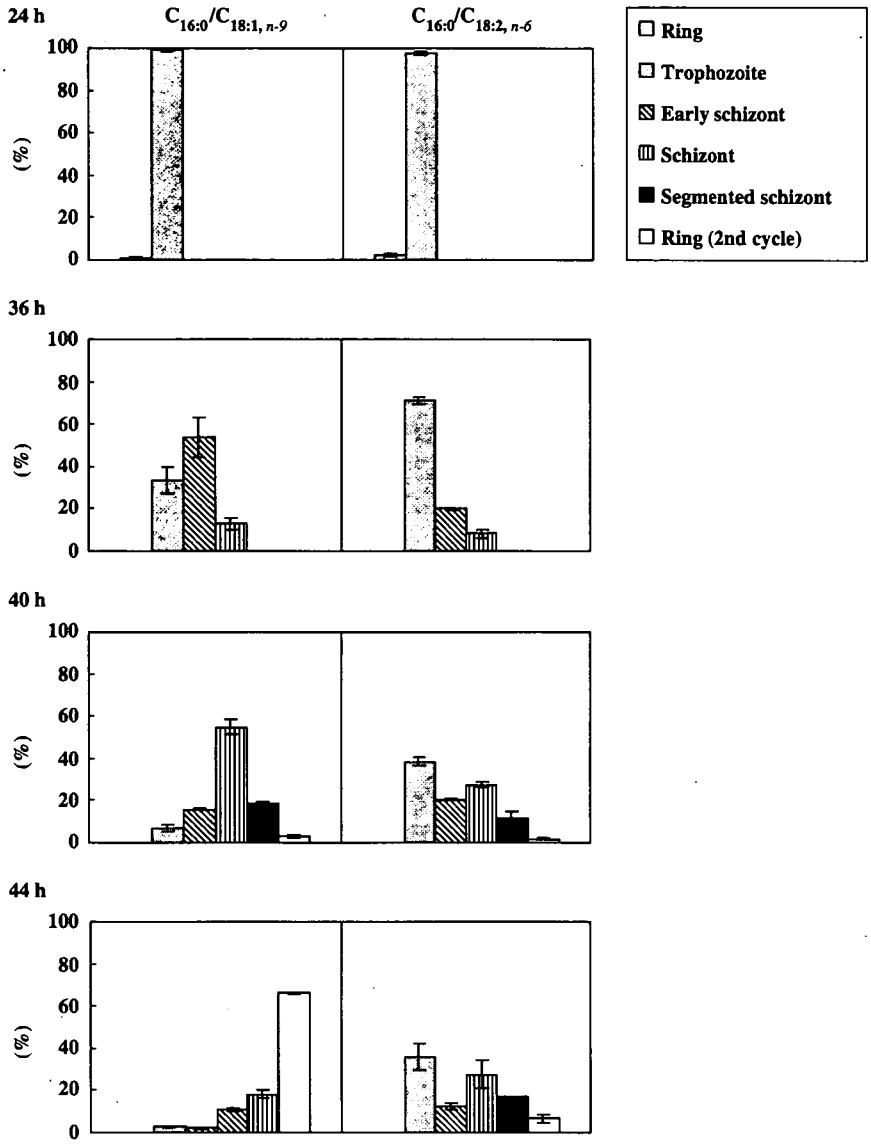

Fig. 6. Distribution of each stage during the course of intraerythrocytic development. Percentages of total parasites at each stage at 24 h, 36 h, 40 h and 44 h are shown. Only the data for parasites of normal appearance from Fig. 5 were used. Results are expressed as a percentage of the parasitaemia at each stage to total parasitaemia at the indicated time. Error bar indicates the difference from the average.

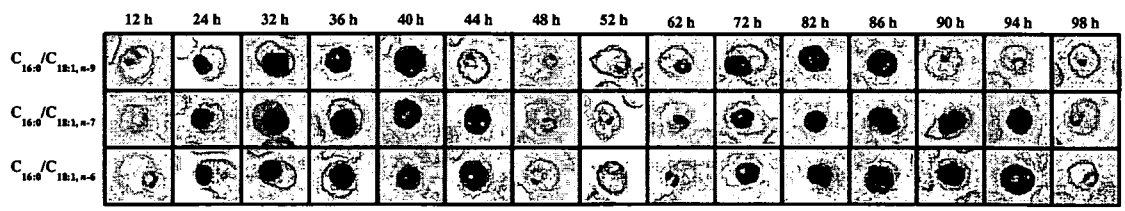

Fig. 7. Morphological changes over time of parasites grown in serum-free medium supplemented with reconstituted lipid-associated BSA containing a combination of fatty acids. Parasite morphology was observed under microscopy on Giemsa-stained slides. Starting parasitaemia was set at 0·13%. The combinations of fatty acids used are indicated at the left side of each row. Final concentrations of fatty acids used were $C_{16:0}/C_{18:1, n-9}$, 30 μM/30 μM; $C_{16:0}/C_{18:1, n-7}$, 30 μM/30 μM; $C_{16:0}/C_{18:2, n-6}$, 30 μM/30 μM.

At 36 h, a slight delay in development was observed in medium containing $C_{16:0}/C_{18:2, n-6}$. At 40 h, decreased synchronicity became remarkable: all stages, with the exception of ring forms, could be seen. At 44 h, the percentage of newly formed rings was much lower than that of trophozoite and schizont,

and the parasites at these mature stages subsequently showed abnormalities in shape, finally becoming pycnotic within the erythrocyte (data not shown). In medium containing $C_{16:0}/C_{18:1,n-9}$, synchronicity was maintained until at least 44 h. At 36 and 40 h, schizont and segmented schizont stages were predominant, and at 44 h, the percentage of newly formed ring stage forms increased as the percentages of the schizont and segmented schizont stages decreased, indicating the onset of the next intraerythrocytic cycle. This interpretation was supported by statistics evaluating the strength of the association of the time and the distribution of stages in each medium containing $C_{16:0}/C_{18:1,n-9}$ or $C_{16:0}/C_{18:2,n-6}$ (Kendall's τ-b: 0·81 in $C_{16:0}/C_{18:1,n-9}$; 0·46 in $C_{16:0}/C_{18:2,n-6}$).

A similar assessment of the effects of $C_{18:1,n-7}$ was performed except that analysis was conducted from 48 h to 100 h, corresponding to the second and transition to the third erythrocytic cycles, during which the growth rate decreased significantly as was seen in medium containing $C_{16:0}/C_{18:2,n-6}$ at 1–52 h. Results obtained in medium containing $C_{16:0}/C_{18:1,n-7}$ were similar to those obtained in medium containing $C_{16:0}/C_{18:2,n-6}$ (data not shown).

We analysed the morphological changes of parasites grown in different serum-free media at the indicated times (Fig. 7). Again we focused only on parasites of normal appearance, and the major morphologies in each sample are shown. In medium containing $C_{16:0}/C_{18:1,n-7}$ or $C_{16:0}/C_{18:2,n-6}$, development proceeded from ring through trophozoite and schizont to segmented schizont, similar to that in medium containing $C_{16:0}/C_{18:1,n-9}$. However, a delay of approximately 4 h was observed. At 36 h, parasites developed into trophozoites, whereas parasites grown in medium containing $C_{16:0}/C_{18:1,n-9}$ reached this stage at 32 h. From 40 to 44 h, parasites grown in medium containing $C_{16:0}/C_{18:1,n-7}$ or $C_{16:0}/C_{18:2,n-6}$ progressed from schizont to segmented schizont, whereas this stage was reached by 36–40 h in medium containing $C_{16:0}/C_{18:1,n-9}$. At 44 h, newly formed rings appeared and were predominant at 52 h in medium containing $C_{16:0}/C_{18:1,n-7}$ or $C_{16:0}/C_{18:2,n-6}$, whereas this stage was reached at 40 h and was predominant at 48 h in medium containing $C_{16:0}/C_{18:1,n-9}$. Thus, we inferred that it takes 44 h and 48 h to complete 1 erythrocytic cycle in medium containing $C_{16:0}/C_{18:1,n-9}$ and $C_{16:0}/C_{18:1,n-7}$ or $C_{16:0}/C_{18:2,n-6}$, respectively.

The results of the present study showed that despite morphological similarities in stage progression, $C_{18:1,n-7}$ or $C_{18:2,n-6}$, when paired with $C_{16:0}$ in serum-free medium, support the growth of only limited populations, resulting in decreased parasitaemias. Given that $C_{18:1,n-9}$, $C_{18:1,n-7}$ and $C_{18:2,n-6}$ differ with respect to the position of the double bond or the degree of unsaturation, it is intriguing that *P. falciparum* differentiates not only the structure of C18 unsaturated fatty acids but also the position of the double bond in C18 monoenoic acids. Taken together, we inferred that $C_{18:1,n-9}$ is indispensable for the intraerythrocytic proliferation of *P. falciparum*.

We thank Ms Hisako Araki for technical assistance and Dr Tetsuya Mizoue for helping statistical analyses. This work was supported by grants from the PRESTO program of the Japan Science and Technology Agency and from the Pharmaceutical and Medical Devices Agency.

REFERENCES

Bhasin, V. K. and Trager, W. (1984). Gametocyte-forming and non-gametocyte-forming clones of *Plasmodium falciparum*. *American Journal of Tropical Medicine and Hygiene* **33**, 534–537.

Hanada, K., Mitamura, T., Fukasawa, M., Magistrado, P. A., Horii, T. and Nishijima, M. (2000). Neutral sphingomyelinase activity dependent on Mg^{2+} and anionic phospholipids in the intraerythrocytic malaria parasite *Plasmodium falciparum*. *The Biochemical Journal* **346**, 671–677.

Holz, G. G. Jr. (1977). Lipids and the malarial parasite. *Bulletin of the World Health Organization* **55**, 237–248.

Maurin, A. C., Chavassieux, P. M., Vericel, E. and Meunier, P. J. (2002). Role of polyunsaturated fatty acids in the inhibitory effect of human adipocytes on osteoblastic proliferation. *Bone* **31**, 260–266. doi:10.1016/S8756-3282(02)00805-0.

Mi-Ichi, F., Kita, K. and Mitamura, T. (2006). Intraerythrocytic *Plasmodium falciparum* utilize a broad range of serum-derived fatty acids with limited modification for their growth. *Parasitology* **133**, 399–410. doi:10.1017/S0031182006000540.

Mitamura, T., Hanada, K., Ko-Mitamura, E. P., Nishijima, M. and Horii, T. (2000). Serum factors governing intraerythrocytic development and cell cycle progression of *Plasmodium falciparum*. *Parasitology International* **49**, 219–229. doi:10.1016/S1383-5769(00)00048-9.

Palacpac, N. M., Hiramine, Y., Mi-Ichi, F., Torii, M., Kita, K., Hiramatsu, R., Horii, T. and Mitamura, T. (2004). Developmental stage-specific triacylglycerol biosynthesis, degradation and trafficking as lipid bodies in *Plasmodium falciparum*-infected erythrocytes. *Journal of Cell Science* **117**, 1469–1480. doi: 10.1242/10.1242/jcs.00988.

Stokes, M. E., Davis C. S. and Koch, G. G. (1995). *Categorical Data Analysis Using the SAS® System*. SAS Institute Inc., Cary, NC.

Surolia, N. and Surolia, A. (2001). Triclosan offers protection against blood stages of malaria by inhibiting enoyl-ACP reductase of *Plasmodium falciparum*. *Nature Medicine* **7**, 167–173. doi:10.1038/84612.

Vial, H. J. and Ancelin, M. L. (1998). Malarial lipids. In Malaria: *Parasite Biology, Pathogenesis, and Protection* (ed. Sherman, I. W.), pp. 159–175. ASM Press, Washington, D.C.

Vial, H. J., Thuet, M. J. and Philippot, J. R. (1982). Phospholipid biosynthesis in synchronous *Plasmodium falciparum* cultures. *The Journal of Protozoology* **29**, 258–263.

Available online at www.sciencedirect.com
ScienceDirect
Molecular & Biochemical Parasitology 151 (2007) 216–219
MOLECULAR & BIOCHEMICAL PARASITOLOGY

Short communication

Cell-free production of functional *Plasmodium falciparum* dihydrofolate reductase-thymidylate synthase

Devaraja G. Mudeppa[a], Cullen K.T. Pang[a], Takafumi Tsuboi[b], Yaeta Endo[b], Fredrick S. Buckner[c], Gabriele Varani[a,d], Pradipsinh K. Rathod[a,*]

[a] *Department of Chemistry, University of Washington, Box 351700, Seattle, WA 98195-1700, USA*
[b] *Cell-free Sciences and Technology Research Center, Ehime University, Bunkyo-cho 3-ban, Matsuyama 790-8577, Japan*
[c] *Department of Medicine, University of Washington, Seattle, WA 98195, USA*
[d] *Department of Biochemistry, University of Washington, Seattle, WA 98195, USA*

Received 29 September 2006; received in revised form 26 October 2006; accepted 26 October 2006
Available online 15 November 2006

Keywords: Malaria; Wheat germ; Protein; Expression; Translation; Enzyme

Malaria continues to burden human populations [1]. The sequencing of several *Plasmodium* genomes has generated much optimism for identification of new drug targets and vaccine candidates [2]. Such efforts should gain considerable traction as the malaria community advances new tools for analyzing gene functions. Of much interest would be a reliable method for producing full-sized, biologically active malaria proteins, particularly when genetic selection schemes are unavailable for sustained production in heterologous systems. Here, we demonstrate that a historically challenging malaria protein, dihydrofolate reductase-thymidylate synthase (DHFR-TS), can be produced cleanly using a wheat germ translation system. In addition to the two catalytic functions, the obligate homodimer also faithfully carries an autologous RNA-binding function. These findings point to new opportunity for expressing functional *Plasmodium falciparum* proteins.

In general, the difficulties of maintaining malaria genes in heterologous systems and of over-expressing *Plasmodium* proteins in functional form started as anecdotes but are now well documented. Out of 1000 *P. falciparum* genes recently transformed into an expression system, two-thirds failed to generate detectable protein [3]. Of the remaining 337 that did, the majority of the protein products were insoluble and not functional.

A detailed examination of difficulties in expressing one pharmacologically important enzyme is revealing. In earlier attempts to overexpress DHFR-TS from *P. falciparum*, several groups learned that heterologous host cells tended to lose full-length malaria coding sequences in the absence of positive selection, presumably to relieve toxicity. The availability of genetic selection for DHFR-TS catalytic functions helped retain full-length DNA sequences but production of active protein was minimal and was frequently accompanied by shorter products derived from internal start sites or premature truncations [4,5]. Purposely truncated DHFR sequences expressed better but often ended up in inclusion bodies [6–8], and of course did not represent full DHFR-TS biochemical functions [9,10]. Fortunately, DHFR-TS biochemistry continued thanks to efficient one-step affinity purification methods for isolating microgram quantities of bioactive protein and sizing columns, which discarded truncated products [4,5,9–11]. Function-based positive genetic selections and affinity columns are not conveniently available for most *P. falciparum* gene products, many of which have unknown functions.

We hypothesized that cell-free transcription-translation systems may be well suited for producing bioactive malaria proteins [12,13]. First, the "host cells" are propagated without *Plasmodium* genes and their products, thus avoiding potentially antiproliferative toxicity. Second, the open nature of cell-free translation systems allows flexibility over reaction conditions (volumes, temperature, kinetics and ingredients) in ways that are unapproachable in living cells, particularly since regulation of *Plasmodium* proteins may involve significant autologous nucleic acid binding functions [10,14]. We chose the wheat germ in vitro translation system, as opposed to the prokaryotic *Escherichia coli* approach or the rabbit reticulocyte system, which is difficult to scale up.

* Corresponding author. Tel.: +1 206 543 1653; fax: +1 206 685 8665.
E-mail address: rathod@chem.washington.edu (P.K. Rathod).

0166-6851/$ – see front matter
doi:10.1016/j.molbiopara.2006.10.016

To appraise the wheat germ system for generating functional *Plasmodium* proteins, we revisited the tough case of *P. falciparum* DHFR-TS. In addition to the empirical challenges mentioned above, this multifunctional product offers significant hurdles in physical assembly. The two separate catalytic domains, DHFR and TS, must be folded correctly. While the DHFR sequence from the amino terminus of the 71 kDa polypeptide can form and function in isolation, the TS active

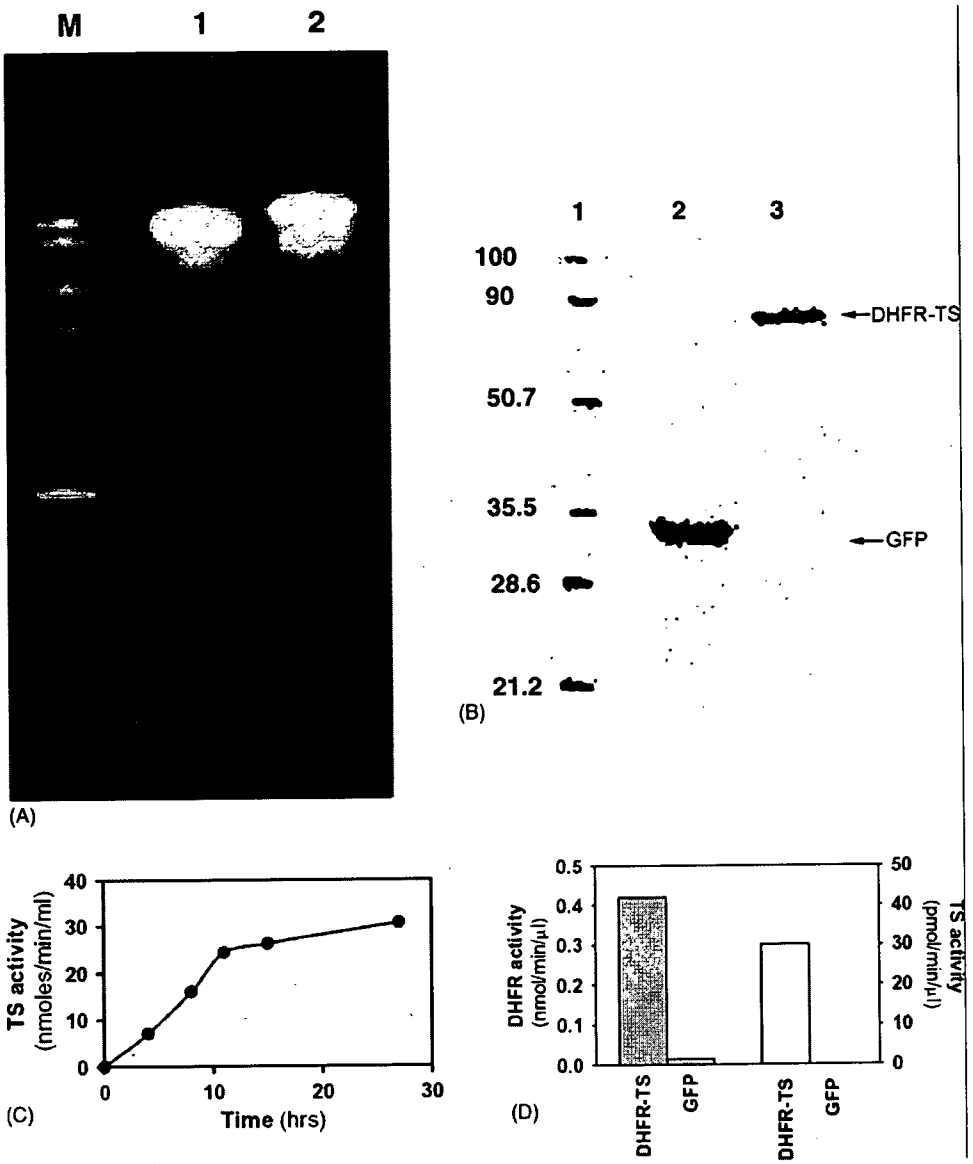

Fig. 1. Cell-free expression of *Plasmodium falciparum* DHFR-TS and its functional characterization. (A) Clean mRNA generated from the transcription of GFP (lane 1) and DHFR-TS (lane 2). Unpurified mRNAs were resolved on 5% urea-polyacrylamide gel and visualized with ethidium bromide. The RNA markers (M) were 2035, 1477, 1199, 707 and 80 bases long. (B) Clean ^{14}C-leucine-labeled DHFR-TS produced in bilayer reaction method. The reaction was carried out as reported [13] with 30 µl of translation mix (lower layer) and 270 µl substrate mix (upper layer) containing 5 kBq (for GFP, lane 2) and 20 kBq (for DHFR-TS, lane 3) of ^{14}C-leucine in U-bottomed 96-well plates. After 18 h of reaction, the lower and upper layers were mixed and 6 µl of sample was applied to a 12% SDS-PAGE before autoradiography. Lane 1 has marker proteins and their molecular weights (kDa) are shown on the left side. (C) Kinetics of *Plasmodium falciparum* DHFR-TS synthesis under dialysis conditions. Reaction samples were assayed after various time intervals for TS activity using a tritium release assay [9]. (D) Two enzyme activities detected in a wheat germ cell-free extract with DHFR-TS mRNA, but not with GFP RNA. Assays for DHFR and TS activity were performed as previously reported [9,11]. (E) mRNA binding activity of cell-free synthesized *Plasmodium falciparum* DHFR-TS. Purified DHFR-TS protein (lanes 1, 3–8; 30 nM) was mixed with 0.35 nM of ^{32}P-labeled DHFR-TS mRNA (lanes 1–8) in the presence, or in the absence, of increasing concentrations (50, 75 and 100 nM) of competing non-labeled DHFR-TS RNA (lanes 3–5) or actin RNA (lanes 6–8). Unbound RNA was digested with RNAse prior to electrophoresis [10]. (F) SDS-PAGE analysis of freshly synthesized GFP and DHFR-TS in crude lysates (lanes 2 and 3, respectively) compared to DHFR-TS purified from a wheat germ reaction (lane 4). After 24 h of translation, lysates were spun for 10 min at 14,000 × *g* and small aliquots (0.8 µl) in the supernatant was loaded on the gel and visualized by CBB stain. For lane 4, DHFR-TS from the translated lysate was purified using methotrexate column followed by gel filtration [9,10]. Lane 1 is marker proteins and their molecular weights (kDa) are shown on the left side.

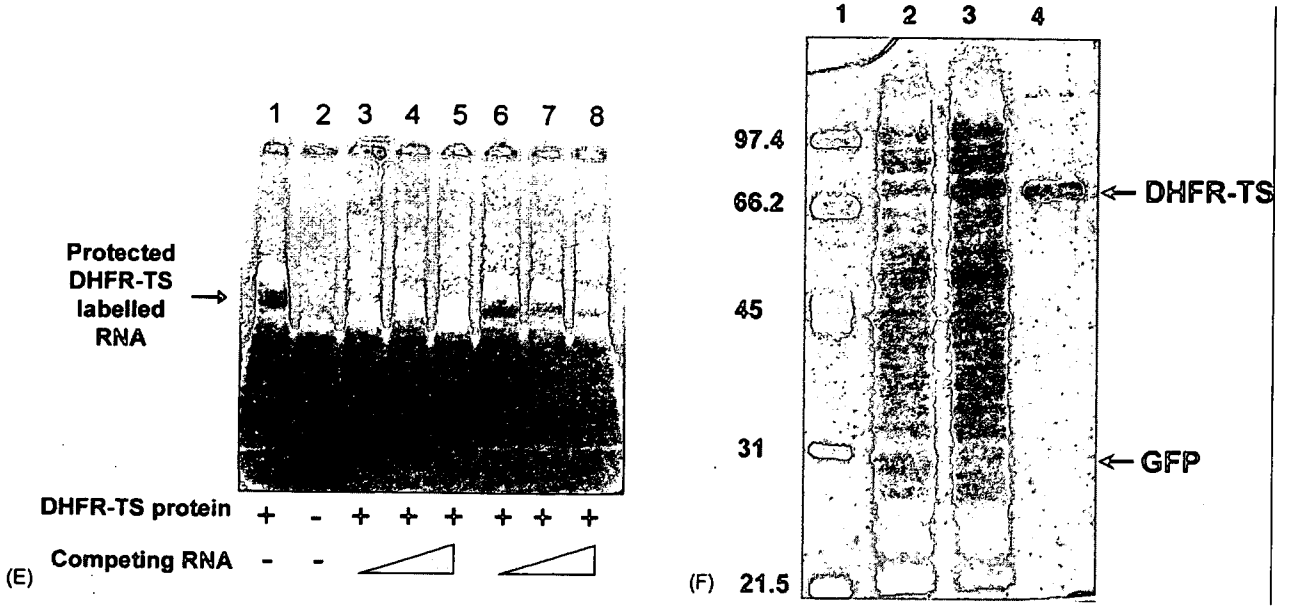

Fig. 1. (*Continued*).

site requires the presence of the DHFR domain [10,14]. Beyond that, an individual TS polypeptide cannot form a functional TS active site. The obligate dimer requires reciprocal contributions from two polypeptides, to assemble each of two TS active sites [15,16]. Finally, PfDHFR-TS has been shown to bind its cognate RNA in a sequence-specific manner but away from the enzyme active sites [10]. Thus, such RNA binding also requires correct assembly and positioning of the multiple domains of DHFR-TS.

For wheat germ expression, the DHFR-TS coding sequence from *P. falciparum* 3D7 was engineered by PCR to have an SP6 RNA polymerase promoter and an Ω sequence for wheat germ ribosome binding site [13]. An RNA transcript was generated using SP6 RNA polymerase (Epicentre, Madison, WI) as previously described [13]. Prior to translation, the quality of the pfDHFR-TS transcript was verified by urea-polyacrylamide gel (Fig. 1A). To evaluate the quality of the translation product from this *P. falciparum* native sequence, protein synthesis was initiated with a wheat germ extract in bilayer mode [13], in the presence of ^{14}C-leucine (American Radiolabeled Chemicals, St. Louis, MO). A single radioactive product with an expected MW of about 71 kDa was observed by SDS-PAGE (Fig. 1B). This demonstrated that the wheat germ system not only used *P. falciparum* AT-rich codons successfully but produced a clean protein product. There was no evidence of excessive fragmentation of template or product, no premature termination of translation and no internal starts within the coding region.

To generate larger quantities of protein, we used a dialysis-based translation protocol, which allows free exchange of fresh reagents around the wheat germ cell lysate, and provides for continual protein synthesis over many hours [17]. Using a longer pEU3b plasmid-derived RNA template, which was expected to last longer, PfDHFR-TS protein synthesis increased linearly for up to 14 h of translation, and continued for another 14 h (Fig. 1C). The majority of the DHFR-TS product was soluble and showed both DHFR and TS catalytic activity (Fig. 1D). RNA protection experiments revealed that the purified DHFR-TS protein, in addition to having DHFR and TS catalytic activity, was capable of binding its cognate RNA (Fig. 1E; Ref. [10]).

By three different criteria, the power of the wheat germ expression system compared favorably against previous approaches. One, based on amounts of DHFR-TS band after SDS-PAGE, we estimated a total yield of about 100 μg of soluble product per milliliter of translation reaction. Two, based on the quality of the functional protein, the cell-free expression appears to be superior. While DHFR activity is a reliable measure of functional protein production, previous experience teaches us that the TS activity is the most labile and a better indicator of well-folded protein. In the present system, we detected 30 nmol/min of TS activity per milliliter of wheat germ extract. Based on a k_{cat} of 120/min for TS (9), this converts to 0.25 nmol (3 μg) of active TS protein per milliliter of extract. This is better than all previous systems where careful efforts were made to measure TS activity, instead of relying on just the stable DHFR activity. Based on TS enzyme activity, this yield of fully functional DHFR-TS protein from 1 ml of wheat germ extract may be comparable to expression from 4500 ml of *P. falciparum* culture [9] or 800 ml of *E. coli* expression using native sequences, albeit under genetic selection [4,5,11]. Three, the present system is the only one that shows production of a distinct DHFR-TS band by Coomassie blue staining (Fig. 1F), a feat not possible even after codon optimized expression in *E. coli* [5]. Even though the wheat germ expression system performs better than other heterologous systems, the amounts of DHFR-TS protein produced is still lower than GFP production (Fig. 1F, lane 2) [12]. The positive control demonstrates that there were no technical difficulties in using the wheat germ extracts [12].

In summary, without genetic selection for function, we have successfully used the wheat germ cell-free protein synthesis sys-

tem to generate bioactive *P. falciparum* DHFR-TS, an obligate dimer with a MW of 142 kDa, four catalytic sites, two different enzyme activities and an RNA binding property. In the face of prior difficulties in producing this protein, the present data offers confidence that the system may find utility in producing many parasite proteins in functional form.

Acknowledgement

The authors are grateful to Dr. Osamu Kaneko (Ehime University) for introducing PKR to the co-authors from Japan. We declare that Dr. Endo has ties to Cell-Free Sciences Co. (http://www.cfsciences.com), which markets wheat germ expression systems. However, all the data presented in this study utilized wheat germ lysates produced in entirety by DGM in the Rathod lab. Neither this study, nor the corresponding author, has received financial benefits from using this expression system. This work was supported by NIH grants (AI26912 and AI60360) and the UW Keck Center for functional genomics. PKR is an Ellison Medical Foundation Senior Scholar in Global Infectious Diseases.

References

[1] Sachs J, Malaney P. The economic and social burden of malaria. Nature 2002;415:680–5.
[2] Gardner MJ, Hall N, Fung E, et al. Genome sequence of the human malaria parasite *Plasmodium falciparum*. Nature 2002;419:498–511.
[3] Mehlin C, Boni E, Buckner FS, et al. Heterologous expression of proteins from *Plasmodium falciparum*: results from 1000 genes. Mol Biochem Parasitol 2006;148:144–60.
[4] Hall SJ, Sims PF, Hyde JE. Functional expression of the dihydrofolate reductase and thymidylate synthetase activities of the human malaria parasite *Plasmodium falciparum* in *Escherichia coli*. Mol Biochem Parasitol 1991;45:317–30.
[5] Prapunwattana P, Sirawaraporn W, Yuthavong Y, Santi DV. Chemical synthesis of the *Plasmodium falciparum* dihydrofolatereductase-thymidylate synthase gene. Mol Biochem Parasitol 1996;83:93–106.
[6] Hekmat-Nejad M, Lee PC, Rathod PK. *Plasmodium falciparum*: direct cloning and expression of pyrimethamine-sensitive and pyrimethamine-resistant dihydrofolate reductase domains. Exp Parasitol 1997;85:303–5.
[7] Sirawaraporn W, Prapuwattana P, Sirawaraporn Y, Yuthavong R, Santi DV. The dihydrofolate reductase domain of *Plasmodium falciparum*. J Biol Chem 1993;268:637–44.
[8] Sano G-I, Morimatsu K, Horii T. Purification and characterization of dihydrofolate reductase of *Plasmodium falciparum* expressed by a synthetic gene in *Escherichia coli*. Mol Biochem Parasitol 1994;63:265–73.
[9] Hekmat-Nejad M, Rathod PK. Kinetics of *Plasmodium falciparum* thymidylate synthase: interactions with high-affinity metabolites of 5-fluoroorotate and D1694. Antimicrob Agents Chemother 1996;40: 1628–32.
[10] Zhang K, Rathod PK. Divergent regulation of dihydrofolate reductase between malaria parasite and human host. Science 2002;296:545–7.
[11] Shallom S, Zhang K, Jiang L, Rathod PK. Essential protein–protein interactions between *Plasmodium falciparum* thymidylate synthase and dihydrofolate reductase domains. J Biol Chem 1999;274:37781–6.
[12] Madin K, Sawasaki T, Ogasawara T, Endo Y. A highly efficient and robust cell-free protein synthesis system prepared from wheat embryos: plants apparently contain a suicide system directed at ribosomes. Proc Natl Acad Sci USA 2000;97:559–64.
[13] Sawasaki T, Gouda MD, Kawasaki T, et al. The wheat germ cell-free expression system: methods for high-throughput materialization of genetic information. Methods Mol Biol 2005;310:131–44.
[14] Mair GR, Braks JA, Garver LS, et al. Regulation of sexual development of Plasmodium by translational repression. Science 2006;313:667–9.
[15] Wattanarangsan J, Chusacultanachai S, Yuvaniyama J, Kamchonwongpaisan S, Yuthavong Y. Effect of N-terminal truncation of *Plasmodium falciparum* dihydrofolate reductase on dihydrofolate reductase and thymidylate synthase activity. Mol Biochem Parasitol 2003;126:97–102.
[16] Yuvaniyama J, Chitnumsub P, Kamchonwongpaisan S, et al. Insights into antifolate resistance from malarial DHFR-TS structures. Nat Struct Biol 2003;10:357–65.
[17] Spirin AS, Baranov VI, Ryabova LA, Ovodov SY, Alakhov YB. A continuous cell-free translation system capable of producing polypeptides in high yield. Science 1988;242:1162–4.

Available online at www.sciencedirect.com
ScienceDirect
Experimental Parasitology 116 (2007) 450–457
Experimental Parasitology
www.elsevier.com/locate/yexpr

Plasmodium berghei XAT: Protective 155/160 kDa antigens are located in parasitophorous vacuoles of schizont-stage parasite

Fumie Kobayashi [a,*], Seiji Waki [b], Mamoru Niikura [c], Mayumi Tachibana [d], Takafumi Tsuboi [e], Motomi Torii [d], Shigeru Kamiya [a]

[a] *Department of Infectious Diseases, Kyorin University School of Medicine, Mitaka, Tokyo 181-8611, Japan*
[b] *Gunma Prefectural College of Health Sciences, Maebashi 371, Japan*
[c] *Institute of Laboratory Animals, Kyorin University School of Medicine, Mitaka, Tokyo, Japan*
[d] *Department of Molecular Parasitology, Ehime University School of Medicine, Shitsukawa Toon, Ehime 791-0295, Japan*
[e] *Cell-Free Science and Technology Research Center, Ehime University, 3 Bunkyo-cho, Matsuyama, Ehime 790-8577, Japan*

Received 23 January 2007; received in revised form 27 February 2007; accepted 27 February 2007
Available online 7 March 2007

Abstract

Effective blood-stage malaria vaccine candidates have been mainly developed from the proteins in exposed locations on the parasite such as the surface of free merozoites or infected red blood cells. In the present study, we identified and localized novel protective antigens derived from the blood-stage of *Plasmodium berghei* XAT after establishment of hybridomas producing protective monoclonal antibodies (mAbs) against the parasites. The protective antigens were expressed in schizonts but not in trophozoites, and located in the parasitophorous vacuoles in the infected erythrocyte cytoplasm. The antigens, with molecular weight of 155/160 kDa, were not identical to any merozoite/schizont antigens that have been reported as target molecules recognized by mAbs developed to rodent malaria parasites. The characterization of new malarial antigenic targets of potentially protective antibody responses following infection would give us new insights for the selection of candidate antigens for malaria vaccine.

Index Descriptors and Abbreviations: *Plasmodium berghei*; Protective immunity; Parasitophorous vacuole; Monoclonal antibody

1. Introduction

Malaria is one of the major infectious diseases for humans in terms of both morbidity and mortality. Every year, it causes 300–500 million new infections and 1–2 million deaths in some 100 countries, with almost half in sub-Saharan Africa (WHO, 1997; Breman, 2001). Despite the enormous efforts to produce a vaccine against malaria, the results to date have not been outstanding (Richie and Saul, 2002). Antigenic diversity and the lack of immunogenicity of vaccine candidates are considered to contribute to the difficulty of developing a successful vaccine. Recently, as one new hope from old ideas, whole parasite approaches using an ultra-low dose of malaria parasites have been shown to be a promising way to induce enhanced immune responses in human and experimental animals (Pombo et al., 2002; Good, 2004; Tongren et al., 2004). These studies suggest that hypervalent subunit vaccines could be much more effective if ideal target antigens are incorporated into them, and has driven us to identify new protective determinants that needed for induction of a maximal immune response in the host.

Plasmodium berghei XAT is an irradiation-induced attenuated variant of the lethal *P. berghei* NK65. Immune competent mice resolve blood-stage *P. berghei* XAT infection following two peaks of parasitemia at about 6 and 13–14 days after inoculation of parasitized red blood cells (PRBC), while parasitemia in mice infected with *P. berghei* NK65 increases progressively and all mice eventually

* Corresponding author. Fax: +81 422 44 4603.
E-mail address: fumfum@kyorin-u.ac.jp (F. Kobayashi).

0014-4894/$ - see front matter © 2007 Elsevier Inc. All rights reserved.
doi:10.1016/j.exppara.2007.02.016

succumb to the infection in 2–3 weeks (Waki et al., 1982). It has been shown that antibody-mediated immunity (Waki, 1994; Waki et al., 1995) as well as cell-mediated immunity (Waki et al., 1992) is important for the resolution of blood-stage *P. berghei* XAT malaria. However, there is no information regarding target molecules responsible for induction of protective antibodies during the infection. In the present study, we identified and localized such molecules derived from the blood-stage of *P. berghei* XAT after establishment of hybridomas producing protective monoclonal antibodies against the parasites.

2. Materials and methods

2.1. Animals

Female BALB/cA Jcl mice were purchased from Clea Japan Inc. (Tokyo, Japan) and were maintained in our animal facility. All animals were 6–8 weeks old at the time of infection.

2.2. Parasite and infection

XAT and NK65 strains of *Plasmodium berghei* were stored as frozen stocks in liquid nitrogen. *P. berghei* XAT is a low-virulence derivative (Waki et al., 1982) from NK65 which is a high-virulence strain and originally obtained from Dr. M. Yoeli of New York University Medical Center. Freshly thawed parasites were passaged once through naive BALB/c mice, and 1×10^4 parasitized erythrocytes from these mice were injected intravenously into experimental mice. Parasitemia was assessed by the microscopic examination of Giemsa-stained smears of tail blood. The percentage of parasitemia was calculated as follows: (number of infected erythrocytes)/(total number of erythrocytes counted) $\times 100 =$ % parasitemia.

2.3. Production of monoclonal antibodies

Plasmodium berghei XAT-parasitized erythrocytes (1×10^4) were injected intravenously into BALB/c mice. Two additional intravenous injections of parasitized erythrocytes (1×10^4 and 2×10^7) were given 11 weeks and 17 weeks after the first injection. Four days after the last injection, spleen cells were harvested and fused with P3-X63-Ag8-U1 (P3U1) mouse myeloma cells using standard hybridoma technology (Mishell and Shiigi, 1980). Briefly, spleen cells and myeloma cells, at a ratio of 3:1, were mixed in the presence of 50% polyethylene glycol 1500 (Boehringer Mannheim, Germany) and grown in 96-well culture plates (Falcon #3072, Becton Dickinson, NJ) containing 200 µl volumes of hypoxanthine-aminopterin-thymidine (HAT)-supplemented RPMI-10S culture medium. The RPMI-10S was supplemented with 10% fetal bovine serum (BioWhittaker, Walkersville, MD.), 20 mM Hepes buffer, 5×10^{-5} M 2-mercaptoethanol, 2.0 mM L-glutamine, 100 U/ml penicillin, and 100 µg/ml streptomycin. The presence of specific antibodies in the hybridoma supernatants was monitored by enzyme linked immunoadsorbent assay (ELISA) on 96-well plates coated with malarial antigens prepared from *P. berghei* XAT or *P. berghei* NK65 as described below. After initial screening, several representative hybridoma cell lines were cloned by two rounds of limiting dilution on feeder layers of BALB/c thymocytes. Selected subclones were expanded for the production of ascites fluid in pristane (2,6,10,14-tetramethylpentadecane) (Sigma Chemical, St. Louis, MO.)-primed mice. Monoclonal antibodies (mAb) were partially purified from ascites fluids by two precipitation steps carried out in 45% saturated ammonium sulfate solution at pH 7.4. Immunoglobulin G (IgG) concentrations were determined by absorbance at 280 nm (OD/1.43).

2.4. Preparation of soluble malarial antigens

The malarial antigens were prepared from the erythrocytic stages. CBA mice were inoculated intravenously with *P. berghei* XAT (1×10^4 parasitized erythrocytes) and anti-IFN-γ mAb (clone: XMG1.5) was administered to infected mice to suppress host protective immunity (Waki et al., 1992). After the mice showed high parasitemia (more than 50%), they were bled by cardiac puncture under ether anesthesia. The heparinized erythrocytes were washed twice in phosphate buffered saline, pH 7.2 (PBS). Then, the cells were passed through a two-layered column composed of 150-210 micron glass beads (Polysciences, Warrington, PA.) and CF11 cellulose (Whatmann International, Maidstone, England) to remove white cells from RBC by the methods of Goldman et al. (1992) with slight modification. After washing twice in phosphate buffered saline, pH 7.2 (PBS), packed cells were diluted to three fold and lysed with an equal volume of 0.1% saponin in PBS. Twenty minutes later, the lysed cells were washed in PBS at least four times. The pellet was diluted to two-fold with PBS and freeze/thawed six times. The preparation was sonicated with UR-200P (Tomy Seiko, Tokyo, Japan) until membranes were disrupted. After centrifugation for 30 min at 40000*g*, the supernatant was collected, filtrated with 0.45 µm filter unit (Millipore, Bedford, MA.) and used as the *P. berghei* XAT-soluble antigens. The *P. berghei* NK65-soluble antigens were prepared in the same manner except the anti-IFN-γ mAb was not administered to infected mice. The crude antigen preparations were stored −80 °C until use. Protein concentration was determined with Bio-Rad reagents (Bio-Rad Laboratories, Richmond, CA) using bovine serum albumin as a standard. Erythrocytes collected from normal and uninfected mice were used for preparation of control soluble antigens.

2.5. Enzyme-linked immunoadsorbent assay (ELISA)

Multi-well plates (96-wells, Sumitomo Bakelite, Tokyo, Japan) were coated with 20 µg/ml of *P. berghei* XAT or NK65 soluble antigens in bicarbonate buffer (pH 9.6)

overnight at 4 °C and subsequently blocked for 2 h at room temperature with 3% skimmed milk (Becton Dickinson, Sparks, MD.) in PBS. After washing three times with PBS containing 0.01% Tween 20 (PBS-T), the plates were dried, wrapped and stored at −34 °C until use. When the presence of specific antibodies in the hybridoma supernatants was monitored, the plates were incubated at room temperature for 1 h with supernatants. After washing three times with PBS-T, the plates were developed with horseradish peroxidase-conjugated goat anti-mouse IgG and IgM (γ, μ and light chain, human IgG absorbed) (BioSource) at dilution of 1:2000. The reactions were visualized by the substrate, 2,2′-azino-bis (3-ethylbenzthiazoline-6-sulfonic acid) (ABTS) (Sigma). For isotype analysis, biotinylated anti-mouse IgG1, IgG2a, IgG2b (Zymed, San Francisco, CA), IgG3 and IgM (Cosmo Bio, Tokyo, Japan) were added to the plates and incubated for 1 h. Then the reactions were visualized by 1 h incubation of the plates with peroxidase conjugated streptavidin (Zymed) and ABTS thereafter. The absorbance of individual wells was determined by using a Microplate Reader MTP-120 (Corona Electric, Ibaraki, Japan) at a wavelength of 415 nm.

2.6. Passive protection assays

Monoclonal antibodies (0.3 mg/head) were administered to mice intraperitoneally on days 0, 1, 4, 5 and 7 relative to infection. On day 0, mice were infected intravenously with 1×10^4 parasitized erythrocytes 1–2 h after the administration of mAb. Percent parasitemias were determined described above.

2.7. Sodium dodecyl sulfate–polyacrylamide gel electrophoresis (SDS–PAGE) and Western blotting

Soluble malarial antigens were denatured in SDS sample buffer (Laemmli, 1970) and proteins were size fractionated under reducing and nonreducing conditions. SDS–PAGE was carried out with a slab gel system according to the method of Laemmli (1970) with a 3% stacking gel and 6% separation gel. After electrophoresis, proteins were transferred to nitrocellulose membranes (Schleicher and Schuell, Dassel, Germany), by the method of Towbin et al. (1979) and the membranes were stained with Ponseau 3R (Sigma) to determine the successful transfer. The membranes were then blocked with PBS containing 1% skimmed milk (PBS-M). Strips were incubated for 1 h at room temperature with mAb (ascites fluids) diluted 1:200 in PBS-M. After extensive washing with PBS-M, the strips were incubated with peroxidase-conjugated rabbit anti-mouse Igs (Dako, Glostrup, Denmark) diluted 1:500 in PBS-M and developed in 0.04% 3,3-diaminobenzidine, tetrahydrochloride (Dojinkagaku Co, Kumamoto, Japan) −0.012% H_2O_2 in PBS-M. Protein weight markers (Bio-Rad, Hercules, CA) were used to determine molecular weights of antigens.

2.8. Indirect immunofluorescent antibody test (IFAT)

Assays were performed according to the method of Takagi et al. (1988). Shortly, infected erythrocytes were collected by intracardiac puncture on heparin, washed twice and diluted with PBS. Thin smears of this parasite suspension were air-dried, fixed with ice-cold acetone, and stored at −80 °C until use. The slides were incubated 30 min with different dilutions of mAb in PBS in a moisture chamber at 37 °C. After three washes in PBS, the slides were incubated 30 min with fluorescein isothiocyatate-conjugated goat anti-mouse IgG plus IgM (Tago, Camarillo, CA) diluted 1:50 in PBS under the same condition as before. The slides were then washed with PBS and mounted under a cover glass with 90% glycerin in bicarbonate buffer and observed with a fluorescence microscope (Olympus, Tokyo, Japan).

2.9. Immunoelectron microscopy

Parasites were fixed for 15 min on ice in a mixture of 1% paraformaldehyde–0.1% glutaraldehyde in 0.1 M phosphate buffer (pH 7.4). Fixed specimens were washed, dehydrated, and embedded in LR White resin (Polysciences, Inc., Warrington, PA) as described previously (Torii et al., 1989; Aikawa and Atkinson, 1990). Thin sections were blocked for 30 min at 37 °C in PBS containing 5% nonfat dry milk and 0.01% Tween 20 (PBS-MT). Grids were then incubated overnight at 4 °C in anti-*P. berghei* XAT mAb or control mAb in PBS-MT. After washing with PBS containing 10% BlockAce (Yukijirushi, Sapporo, Japan) and 0.01% Tween 20 (PBS-BT), the grids were incubated for 1 h at 37 °C with goat anti-mouse IgG conjugated to gold particles (Amersham Life Science, Arlington, IL) diluted 1:20 in PBS-MT, rinsed with PBS-BT, and fixed on ice for 10 min in 2.5% glutaraldehyde to stabilize the gold. Then the grids were rinsed with distilled water, dried, and stained with uranyl acetate and lead citrate. Samples were examined with a Hitachi H-800 electron microscope.

3. Results

3.1. Development of hybridomas

Spleen cells from mice immunized with *P. berghei* XAT were fused with mouse myeloma cells (P3-X63-Ag8-U1) 4 days after the last inoculation of parasitized erythrocytes. By day 18 after the fusion, hybridomas were detected in 703 out of 1440 wells (48.8%) and the supernatants were screened by ELISA utilizing 96-well plates coated with soluble antigens extracted from *P. berghei* XAT. Eighty-two wells (11.7%) were positive for anti-*P. berghei* XAT antibody production. Several hybridoma lines secreting high titers of antibodies were cloned by limiting dilution on thymocyte feeder layers, and eventually, seven hybridoma clones were selected and re-cloned. In ELISA for screening, three out of 7 mAbs (A1C9, G1D2 and B1B10) reacted

strongly with the soluble extracts of both *P. berghei* XAT and NK65, but the reactivity of 4 mAbs (C11F12, H6G11, B1D6 and A1A5) against *P. berghei* NK65 antigens was much weaker than XAT (data not shown). The isotypes of mAbs were determined by *P. berghei* XAT antigen-coated ELISA plates using class and subclass-specific antisera. MAbs H6G11 and B1D6 were identified as IgG1, and the remaining mAbs were IgM classes.

3.2. Passive protection tests with monoclonal antibodies

To determine the extent to which passively transferred mAbs might influence the course of infection of *P. berghei* XAT, groups of BALB/c mice were treated with 7 mAbs selected as above on days 0, 1, 4, 5 and 7 after infection with 1×10^4 parasitized erythrocytes (Fig. 1). When PBS was administered as controls, two of three mice had two peaks of parasitemia on days 6 and 14 (the mean was 2.20% and 6.45%, respectively) after the parasite inoculation then suppressed the parasitemia spontaneously. Unexpectedly, the reminder showed a progressively increasing parasitemia after the first peak and died on day 24 of infection, suggesting that *P. berghei* XAT parasite had reverted to the virulent *P. berghei* NK65 phenotype in some mice. The course of parasitemia in groups of mice receiving mAbs A1A5, A1C9, B1B10, C11F12 and G1D2, all of which were identified as IgM, was similar to that in PBS-treated mice. In contrast, mice given mAb B1D6 had extre-

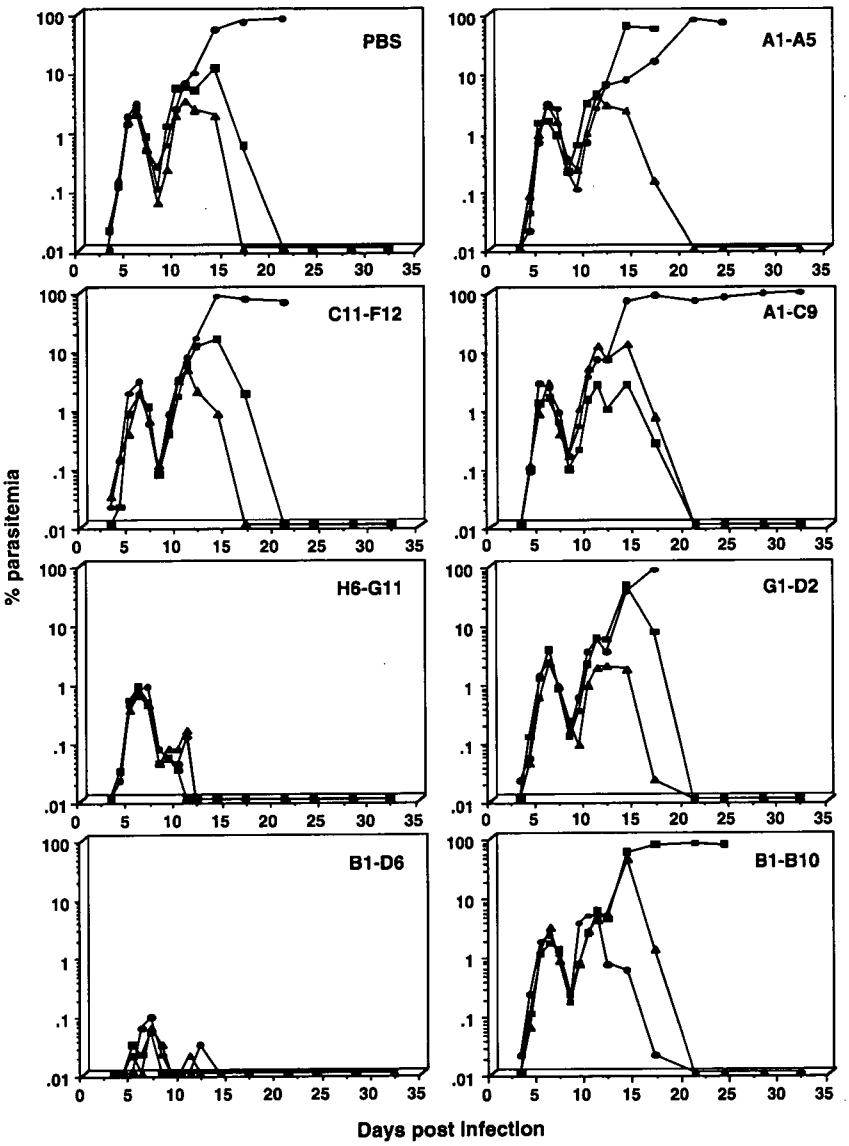

Fig. 1. Courses of infection of *Plasmodium berghei* XAT in BALB/c mice treated with 7 monoclonal antibodies. MAbs (0.3 mg/head) were administered to mice intraperitoneally on days 0, 1, 4, 5 and 7 relative to infection. Control mice received PBS. On day 0, mice were infected intravenously with 1×10^4 parasitized erythrocytes 1–2 h after the administration of mAb. The parasitemias were determined by examination of Giemsa-stained thin blood smears.

mely low levels of parasitemia during infection. The average parasitemia was 0.07% even in the peak on day 7 and did not exceed 0.01% from day 9 after infection. The administration of mAb H6G11 also affected the kinetics of infection. Although the mean parasitemia reached peak values of 0.7% on day 7, it declined to less than 0.01% by day 12 of infection in mAb H6G11-treated mice (Fig. 1). The subclasses of protective mAbs were IgG1. From these results, further experiments were performed mainly using mAb B1D6.

To determine whether the protection by the mAb B1D6 was specific, an irrelevant IgG1 mAb was administered to groups of five mice and their parasitemia was compared with mAb B1D6-treated mice by the same protocols described above. Mice that were infected with *P. berghei* XAT and received the irrelevant IgG1 mAb had almost the same course of infection as PBS-treated mice. The administration of mAb B1D6, again, suppressed the development of parasitemia, confirming that this protection was specific for the antibody against malarial antigen (Fig. 2).

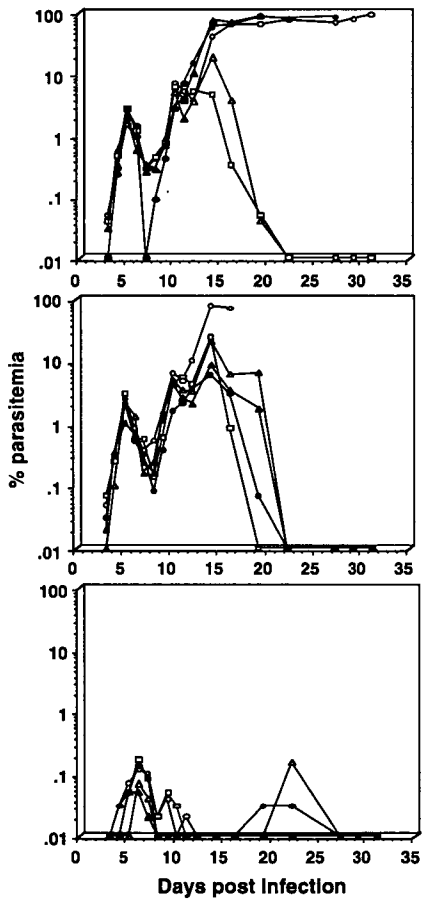

Fig. 2. Courses of infection of *P. berghei* XAT in BALB/c mice treated with mAb B1D6. The mAb B1D6 (0.3 mg/head) was administered to mice intraperitoneally on days 0, 1, 4, 5 and 7 relative to infection. Control mice received PBS or an irrelevant mAb of identical IgG1 isotype (0.3 mg/head). On day 0, mice were infected intravenously with 1×10^4 parasitized erythrocytes 1–2 h after the administration of mAb. The parasitemias were determined by examination of Giemsa-stained thin blood smears. (upper) PBS, (middle) an irrelevant IgG1 mAb, (lower) mAb B1D6.

3.3. Molecular weight of the target antigens

The target antigens recognized by mAb B1D6 were characterized by Western blot analysis (Fig. 3). Soluble malarial antigens extracted from *P. berghei* XAT were electrophoresed by SDS–PAGE and transferred to nitrocellulose membranes. Polyclonal hyper-immune sera against soluble malarial antigens reacted with at least 20 polypeptides, varying in molecular weight from 20 to 250 kDa (Fig. 3, lane A). In contrast, mAb B1D6 strongly reacted with two molecules with molecular sizes close to each other (Fig. 3, lane B) with molecular weights of 155 and 160 kDa. An irrelevant IgG1 mAb as control did not react with any bands (data not shown).

3.4. Stage-specific and species-specific parasite recognition by protective mAb

Stage, strain, and species specificity and localization of the target antigens recognized by mAb B1D6 were determined by IFAT and DAPI staining on fixed thin blood films prepared from mice infected with *P. berghei* XAT (Fig. 4). The staining with DAPI showed numbers of the

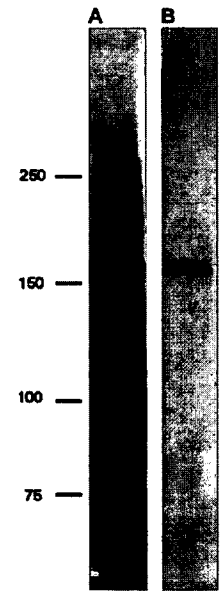

Fig. 3. Western blot analyses of antigens of *P. berghei* XAT with mAbs B1D6. Malarial antigens (50 μg) were separated by SDS–PAGE (6% gels) under reducing conditions and transferred to nitrocellulose membranes. The blots were probed with the polyclonal hyper immune serum (1:500) (lane A) and mAb B1D6 (ascites fluids, 1:200) (lane B) and incubated with peroxidase-conjugated rabbit anti-mouse Igs. Subsequently, immunoreactive bands were visualized with 3,3′-diaminobenzidine, tetrahydrochloride. An irrelevant IgG1 mAb as control did not react with any bands. The sizes of the prestained molecular weight markers (in kilodaltons) are shown to the left of the gels.

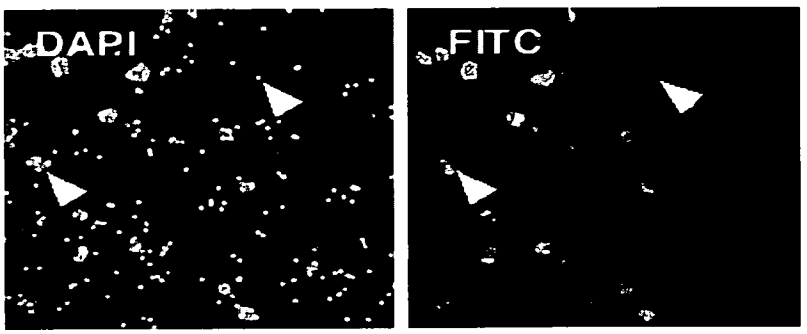

Fig. 4. Indirect immunofluorescence staining of *P. berghei* XAT with mAb B1D6. Malarial parasites were fixed and stained with DAPI (left panel) or incubated with mAb B1D6 and reacted with FITC-conjugated anti-mouse Ig (right panel). The arrowheads in left panel indicate a trophozoite (small dot) and a schizont (large one). Note that schizonts are strongly positive but trophozoites are negative. An irrelevant IgG1 mAb as control did not react with any stages of malaria parasites.

erythrocytic cycles and free merozoites of *P. berghei* XAT in a field. MAb B1D6 reacted with schizonts but not with trophozoites (Fig. 4). The epitopes recognized by mAb B1D6 were also found in a schizont of the parent strain, *P. berghei* NK65, but the mAb did not react with blood-stage *P. yoelii* or *P. falciparum* (data not shown).

3.5. Immunoelectron microscopic localization of target antigens recognized by protective mAb

Cellular localization of epitopes recognized by mAb B1D6 was further examined by immunoelectron microscopy. Gold particles showing the epitopes were detectable in early (Fig. 5A) and mature schizont-stage parasites (Fig. 5B). There were no free merozoites and trophozoites showing the deposition of gold particles (data not shown). The target antigens recognized by mAb B1D6 were localized in the parasitophorous vacuoles and in the clefts in the infected erythrocyte cytoplasm.

4. Discussion

The aim of this study was to produce protective mAbs against the *P. berghei* XAT, to characterize the mAbs with regard to the effect on the course of infection and to specify and localize the target antigens. We firstly established seven clones of hybridoma producing mAbs that strongly reacted with determinants on antigens of erythrocytic stages of the parasite in ELISA. When two of these mAbs, B1D6 and H6G11, were passively administered to BALB/c mice on and after infection, they dramatically inhibited the course of infection initiated with *P. berghei* XAT. Takagi et al. (1988) reported the establishment of specific mAb recognizing a 240-kDa molecule on the schizont stages of *P. berghei*

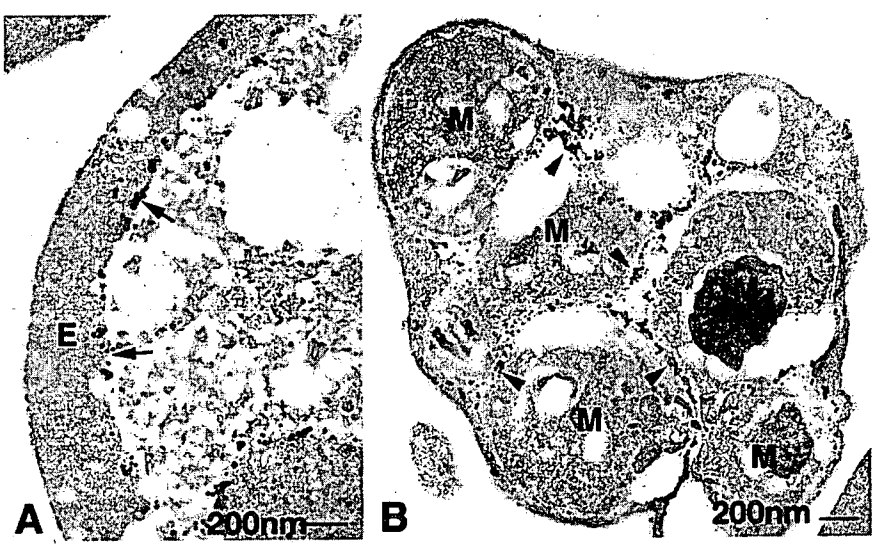

Fig. 5. Immunoelectron micrographs of erythrocytes infected with *P. berghei* XAT early schizont (A) and mature schizont (B) that were incubated with mAb B1D6. E, erythrocyte; M, merozoite. Note that gold particles were associated with the parasitophorous vacuole space and in the clefts (arrows). Bar = 200 nm.

XAT. Whether their mAb had a protective role was not determined. Their mAb did not react with *P. berghei* NK65, suggesting that the epitopes could become a marker of attenuated *P. berghei*. In the present study, the low reactivity of protective mAb B1D6 to the extracts of *P. berghei* NK65 in ELISA, which had been performed for screening, made us expect that our mAb also recognized *P. berghei* XAT-specific antigens. The mAb B1D6, however, reacted with schizont stages in the blood of mice infected with *P. berghei* NK65 as well as XAT in IFAT, indicating that the epitopes were not attenuated-variant specific. The discrepancy between these results could be attributed to the different percentages of target antigens in total parasite proteins. The protective mAb B1D6 appears to be species-specific as it did not react with the blood-stage *P. yoelii* or *P. falciparum* in IFAT.

The course of infection with *P. berghei* XAT is characterized by two peaks of parasitemia: the first small peak within a week and the second large peak around 2 weeks after infection. It has been suggested that two different mechanisms contribute to the protection against *P. berghei* XAT. During early phase of infection, antibody-dependent neutrophil-mediated killing (Waki et al., 1993; Waki, 1994) and effector cells such as macrophages which are activated by IFN-γ (Yoneto et al., 2001) have been shown to play major roles for the suppression of development of the parasites. These mechanisms, however, do not appear to be efficient enough to eliminate all parasites from the blood. In the later phase of infection, specific IgG2a isotype plays dominant role in mediating immunity to induce recovery from the infection (Waki et al., 1995) in a similar manner to rodent malarias caused by *P. yoelii* (White et al., 1991), *P. vinckei* (Finnemann et al., 1992) and *P. chabaudi* (von der Weid et al., 1994). Therefore, it is of interest that mAb B1D6 suppressed parasitemia in both the first peak and second peak. MAb B1D6 could be involved in immunity to both early and later phases of infection. Moreover, the protective mAbs B1D6 and H6G11 had an unusual isotype, IgG1. The findings of protective IgG1 mAb during *P. berghei* XAT infection support the argument by others that protective activity is not restricted to one IgG subclass (Majarian et al., 1984).

How mAb B1D6 interacts with blood-stage parasites and reduces the level of parasitemia remains unknown. Although the proteins recognized by this mAb were abundantly expressed in the parasitophorous vacuole space (Fig. 5), there was no evidence that they were expressed on the surface of infected erythrocytes or of free merozoites. The serine-repeat antigen (SERA) is one of the vaccine candidate antigens against the asexual blood stage of *P. falciparum*. The 126-kDa SERA proteins accumulate in the parasitophorous vacuole in the late trophozoite and schizont stages (Banyal and Inselburg, 1985; Bzik et al., 1988; Delplace et al., 1987). Pang et al. (1999) observed that antibodies against SERA N-terminal-domain protein bound to the rupturing schizont but not to membrane of schizont-infected RBC. Since each merozoite would be released after breaking of both RBC and parasitophorous vacuole membrane, they postulated that their antibody could invade the parasitophorous vacuole and cross-link merozoites when infected RBC at schizont stage began to rupture. It is probable that mAb B1D6 prevents the release of merozoites and then causes parasite growth inhibition in the same manner as they proposed since the target antigens recognized by mAb B1D6 were observed around each merozoite in a schizont-infected RBC as reported for SERA.

The effective component in malaria vaccines has been considered to be proteins in exposed locations on the parasite such as the merozoite surface and the surface of the infected red blood cells (Holder, 1996). Indeed, the asexual-blood-stage target antigen that is undergoing the most intensive investigation is still the merozoite surface protein, MSP-1 (Target, 2005). We showed here that it is possible that proteins mainly located in the parasitophorous vacuole could be effective vaccine candidates. Further studies are necessary to examine the role of the proteins recognized by the mAb B1D6 in immune responses of the host and to develop the genomic and proteomic data since this would be helpful for the development of effective vaccines.

Acknowledgments

This work was supported in part by a Grant-in-Aid for Scientific Research on Priority Areas from the Ministry of Education, Science, Sports and Culture in Japan and a Grant-in-Aid for Scientific Research (C) from Japan Society for the Promotion of Science to F.K.

References

Aikawa, M., Atkinson, C.T., 1990. Immunoelectron microscopy of parasites. Advances in Parasitlogy 29, 151–214.

Banyal, J.S., Inselburg, J., 1985. Isolation and characterization of parasite-inhibitory *Plasmodium falciparum* monoclonal antibodies. The American Journal of Tropical Medicine and Hygiene 34, 1055–1064.

Breman, J.G., 2001. The ears of the hippopotamus: manifestations, determinants, and estimates of the malaria burden. The American Journal of Tropical Medicine and Hygiene 64 (Suppl. 1–2), 1–11.

Bzik, D.J., Li, W.-B., Horii, T., Inselburg, J., 1988. Amino acid sequence of the serine-repeat antigen (SERA) of *Plasmodium falciparum* determined from cloned cDNA. Molecular and Biochemical Parasitology 30, 279–288.

Delplace, P., Fortier, B., Tronchin, G., Dubremetz, J.-F., Vernes, A., 1987. Localization, biosynthesis, processing and isolation of a major 126 kDa antigen of the parasitophorous vacuole of *Plasmodium falciparum*. Molecular and Biochemical Parasitology 23, 193–201.

Finnemann, S., Kremsner, P.G., Chaves, M.F., Schumacher, C., Neifer, S., Bienzle, U., 1992. Antibody response in *Plasmodium vinckei* malaria after treatment with chloroquine and adjuvant interferon-gamma. Parasitology Research 78, 629–634.

Goldman, I.F., Qari, S.H., Skinner, J., Oliveira, S., Nascimento, J.M., Povoa, M.M., Collins, W.E., La, A.A., 1992. Use of glass beads and CF11 cellulose for removal of leukocytes from malaria-infected human blood in field setting. Memorias dó Instituto Oswaldo Cruz 87, 583–587.

Good, M.F., 2004. Vaccine-induced immunity to malaria parasites and the need for novel strategy. Trends in Parasitology 21, 29–34.

Holder, A.A., 1996. Preventing merozoite invasion of erythrocytes. In: Hoffman, S.L. (Ed.), Malaria Vaccine Development. ASM Press, Washington, DC, pp. 77–104.

Laemmli, U.K., 1970. Cleavage of structural proteins during the assembly of the head of bacteriophage T4. Nature 227, 680–685.

Majarian, W.R., Daly, T.M., Weidanz, W.P., Long, C.A., 1984. Passive immunization against murine malaria with an IgG3 monoclonal antibody. Journal of Immunology 132, 3131–3137.

Mishell, B.B., Shiigi, S.M., 1980. Immunoglobulin producing hybrid cell lines. In: Mishell, B.B., Shiigi, S.M. (Eds.), Selected Methods in Cellular Immunology. W. H. Freeman and Company, San Francisco, pp. 351–372.

Pang, X.-L., Mitamura, T., Horii, T., 1999. Antibodies reactive with the N-terminal domain of *Plasmodium falciparum* serine repeat antigen inhibit cell proliferation by agglutinating merozoites and schizonts. Infection and Immunity 67, 1821–1827.

Pombo, D.J., Lawrence, G., Hirunpetcharat, C., Rzepczyk, C., Bryden, M., Cloonan, N., Anderson, K., Mahakunkijcharoen, Y., Martin, L.B., Wilson, D., Elliott, S., Elliott, S., Eisen, D.P., Weinberg, J.B., Saul, A., Good, M.F., 2002. Immunity to malaria after administration of ultra-low doses of red cells infected with *Plasmodium falciparum*. Lancet 360, 610–617.

Richie, T.L., Saul, A., 2002. Progress and challenges for malaria vaccine. Nature 415, 694–701.

Takagi, T., Waki, S., Kogure, S., Sugioka, Y., Suzuki, M., 1988. A marker epitope of attenuated *Plasmodium berghei*. Parasitology Research 74, 436–440.

Target, G.A., 2005. Malaria vaccines 1985–2005: a full circle? Trends in Parasitology 21, 499–503.

Tongren, E.J., Zavala, F., Roos, D.S., Riley, E.M., 2004. Malaria vaccines: if at first you don't succeed. Trends in Parasitology 20, 604–610.

Torii, M., Adams, J.H., Aikawa, M., 1989. Release of merozoite dense granules during erythrocyte invasion by *Plasmodium knowlesi*. Infection and Immunity 57, 3230–3233.

Towbin, M., Staehelin, T., Gordon, J., 1979. Western blotting: electrophoretic transfer of proteins from sodium sulfate–polyacrylamide gels to unmodified nitrocellulose and radiographic detection with antibodies and radio-iodinated proteins. Proceedings of the National Academy of Sciences of the United States of America 76, 4350–4354.

von der Weid, T., Kopt, M., Kohler, G., Langhorne, J., 1994. The immune response to *Plasmodium chabaudi* malaria in interleukin-4-deficient mice. European Journal of Immunology 24, 2285–2293.

Waki, S., 1994. Antibody-dependent neutrophil-mediated parasite killing in non-lethal rodent malaria. Parasite Immunology 16, 587–591.

Waki, S., Kurihara, R., Nemoto, H., Suzuki, M., 1993. Effect of recombinant human colony-stimulating factor on the course of parasitaemia in non-lethal rodent malaria. Parasitology Research 79, 703–705.

Waki, S., Tamura, J., Imanaka, M., Ishikawa, S., Suzuki, M., 1982. *Plasmodium berghei:* isolation and maintenance of an irradiation attenuated strain in the nude mouse. Experimental Parasitology 53, 335–340.

Waki, S., Uehara, S., Kanbe, K., Nariuchi, H., Suzuki, M., 1995. Interferon-gamma and the induction of protective IgG2a antibodies in non-lethal *Plasmodium berghei* infections of mice. Parasite Immunology 17, 503–508.

Waki, S., Uehara, S., Kanbe, K., Ono, K., Suzuki, M., Nariuchi, H., 1992. The role of T cells in pathogenesis and protective immunity to murine malaria. Immunology 75, 646–651.

White, W.I., Evans, C.B., Taylor, D.W., 1991. Antimalarial antibodies of the immunoglobulin G2a isotype modulate parasitaemia in mice infected with *Plasmodium yoelii*. Infection and Immunity 59, 3547–3554.

World Health Organization, 1997. Weekly Epidemiological Record, World malaria situation in 1994—Part I, 72, 269–274.

Yoneto, T., Waki, S., Takai, T., Tagawa, Y-i., Iwakura, Y., Mizuguchi, J., Nariuchi, H., Yoshimoto, T., 2001. A critical role of Fc receptor-mediated antibody-dependent phagocytosis in the host resistance to blood-stage *Plasmodium berghei* XAT infection. Journal of Immunology 166, 6236–6241.

JOURNAL OF CLINICAL MICROBIOLOGY, Aug. 2007, p. 2521–2528 Vol. 45, No. 8
0095-1137/07/$08.00+0 doi:10.1128/JCM.02117-06

Detection of Four *Plasmodium* Species by Genus- and Species-Specific Loop-Mediated Isothermal Amplification for Clinical Diagnosis[▽]

Eun-Taek Han,[1,2] Risa Watanabe,[1] Jetsumon Sattabongkot,[3] Benjawan Khuntirat,[3] Jeeraphat Sirichaisinthop,[4] Hideyuki Iriko,[5] Ling Jin,[5] Satoru Takeo,[1] and Takafumi Tsuboi[1,5]*

Cell-Free Science and Technology Research Center[1] and Venture Business Laboratory,[5] Ehime University, Matsuyama, Ehime 790-8577, Japan; Department of Parasitology, Kangwon National University College of Medicine, Chunchon 200-701, Korea[2]; Department of Entomology, Armed Forces Research Institute of Medical Sciences, Bangkok 10400, Thailand[3]; and Vector Borne Disease Training Center, Pra Budhabat, Saraburi 18120, Thailand[4]

Received 16 October 2006/Returned for modification 6 December 2006/Accepted 31 May 2007

Loop-mediated isothermal amplification (LAMP), a novel nucleic acid amplification method, was developed for the clinical detection of four species of human malaria parasites: *Plasmodium falciparum*, *P. vivax*, *P. malariae*, and *P. ovale*. We evaluated the sensitivity and specificity of LAMP in comparison with the results of microscopic examination and nested PCR. LAMP showed a detection limit (analytical sensitivity) of 10 copies of the target 18S rRNA genes for *P. malariae* and *P. ovale* and 100 copies for the genus *Plasmodium*, *P. falciparum*, and *P. vivax*. LAMP detected malaria parasites in 67 of 68 microscopically positive blood samples (sensitivity, 98.5%) and 3 of 53 microscopically negative samples (specificity, 94.3%), in good agreement with the results of nested PCR. The LAMP reactions yielded results within about 26 min, on average, for detection of the genus *Plasmodium*, 32 min for *P. falciparum*, 31 min for *P. vivax*, 35 min for *P. malariae*, and 36 min for *P. ovale*. Accordingly, in comparison to the results obtained by microscopy, LAMP had a similar sensitivity and a greater specificity and LAMP yielded results similar to those of nested PCR in a shorter turnaround time. Because it can be performed with a simple technology, i.e., with heat-treated blood as the template, reaction in a water bath, and inspection of the results by the naked eye because of the use of a fluorescent dye, LAMP may provide a simple and reliable test for routine screening for malaria parasites in both clinical laboratories and malaria clinics in areas where malaria is endemic.

The rapid and accurate diagnosis of malaria presents a challenge in most countries where it is endemic. Of the four *Plasmodium* species, *Plasmodium falciparum*, infection with which can be fatal, must be identified promptly and differentiated from the other *Plasmodium* species that produce human disease (12). In addition, most regions where malaria is endemic feature infections involving two or more of these species; these mixed infections often go unrecognized or underestimated (30). Failure to detect mixed infections could result in inadequate or incorrect treatment and may result in severe disease (11). There is therefore an urgent need to develop diagnostic methods that are simple, sensitive, and species specific.

Currently, the conventional method for the diagnosis of malaria is microscopic examination of thin and/or thick blood smears. Although light microscopy has a relatively high sensitivity and specificity and also provides parasite density, the stage, and species differentiation, this method is labor-intensive, requires well-trained experts, and may result in therapeutic delays. To improve the speed and precision of malaria diagnosis in areas where standard laboratory diagnosis is not available, researchers have developed malaria rapid diagnostic tests based on antigen-capture immunochromatographic technologies (12, 16). When they are in good condition, some products can achieve sensitivity for the detection of *P. falciparum* infection similar to that of expert microscopists (3, 10). However, the sensitivity can vary between products (14), and a species-specific product is available only for *P. falciparum*. Very long observation times and considerable expertise are required for a correct diagnosis by microscopy under several circumstances: when the level of parasitemia is low, during mixed infection, after drug treatment, and during the chronic phase of the infection. Therefore, this situation can lead to false-negative results or unreliable species determinations (1).

Subsequently, molecular methods based on DNA amplification, such as nested PCR and real-time quantitative PCR, were developed for the diagnosis of malaria. Compared to microscopy, these methods have demonstrated higher sensitivity, detecting one to five parasites/μl of blood, and greater specificity for mixed infection (7, 19, 22, 24–27). However, the long turnaround time, high cost, and availability only in well-equipped laboratories render this technology inadequate for routine diagnosis in hospital laboratories and field clinics in areas where malaria is endemic (4).

Recently, a new, rapid, simple, and sensitive technique called loop-mediated isothermal amplification (LAMP) was developed (17). LAMP is a nucleic acid amplification method that relies on autocycling strand-displacement DNA synthesis performed with Bst DNA polymerase. The amplification products are stem-loop DNA structures with several inverted repeats of the target and structures with multiple loops. The

* Corresponding author. Mailing address: Cell-Free Science and Technology Research Center, Ehime University, Matsuyama, Ehime 790-8577, Japan. Phone: 81-89-927-8277. Fax: 81-89-927-9941. E-mail: tsuboi@ccr.ehime-u.ac.jp.

▽ Published ahead of print on 13 June 2007.

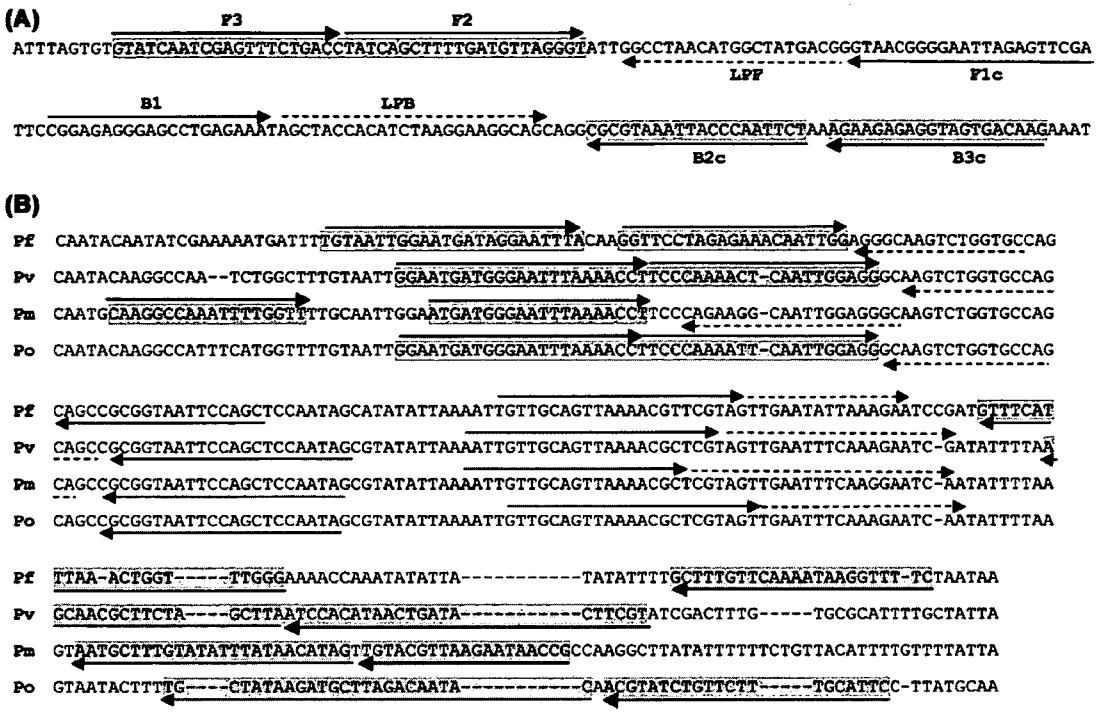

FIG. 1. Location and sequence of LAMP targets and priming sites for *Plasmodium* genus (A) and four *Plasmodium* species (B). (A) The locations of the priming sites by the *Plasmodium* genus-specific primer set in the reference sequence (GenBank accession no. M19173.1) are indicated by arrows. (B) Partial sequence alignment of the 18S rRNA genes of four human malaria parasites, *P. falciparum* (Pf; GenBank accession no. M19173.1), *P. vivax* (Pv; GenBank accession no. U03079), *P. malariae* (Pm; GenBank accession no. M54897), and *P. ovale* (Po; GenBank accession no. L48986), along with the species-specific primer annealing sites.

principal merit of this method is that no denaturation of the DNA template is required (15), and thus, the LAMP reaction can be conducted under isothermal conditions (ranging from 60 to 65°C). LAMP requires only one enzyme and four primers that recognize six distinct target regions. The method produces a large amount of amplified product, resulting in easier detection, such as detection by visual judgment of the turbidity or fluorescence of the reaction mixture (13).

Several investigators have reported on LAMP methods for the rapid identification of *Plasmodium*, *Trypanosoma*, and *Babesia* and have commended the usefulness of the LAMP assay (5, 8, 21, 29). Poon et al. estimated that the cost of running a LAMP assay is about 1/10 of that of the normal PCR method for *P. falciparum* detection (21). The biggest reduction in cost and time came from simple sample preparation, with no requirement for previous DNA extraction (6). Briefly, simple heating of the infected blood at 99°C for 10 min was enough to prepare the DNA template for LAMP without any inhibition of the reaction (21). However, to date, the use of LAMP for the detection of malaria parasites for clinical diagnosis has been validated only with acute falciparum malaria patients (21). Although *P. falciparum* is the most important cause of severe disease, its geographic distribution overlaps those of *P. vivax*, *P. malariae*, and *P. ovale*; and therefore, a method that allows the rapid detection and identification of all four species infecting humans would be preferable.

In the present study, we describe a LAMP for the clinical detection and identification of *P. falciparum*, *P. vivax*, *P. malariae*, and *P. ovale*. The technique was evaluated with blood samples obtained from field clinics. The results of LAMP were compared to those of conventional microscopy and nested PCR.

MATERIALS AND METHODS

Patient samples. Sixty-eight samples that were positive for malaria parasites by microscopy were collected from the malaria clinics of Mae Sod and Mae Kasa in northwestern Thailand. In addition, 53 samples that were negative by microscopy were collected from Kong Mong Tha, a village in Kanchanaburi Province in western Thailand. The blood samples were tested by nested PCR and LAMP. Each of the molecular tests was carried out and interpreted by independent researchers (nested PCR at the Armed Forces Research Institute of Medical Sciences, Thailand, and LAMP at the Cell-Free Science and Technology Research Center, Ehime University, Japan) blinded to the origins of the specimens and the laboratory results.

Conventional microscopy. Thick blood smears were examined under ×1,000 magnification by microscopists with extensive experience in the identification of malaria parasites. The parasite density per 500 leukocytes was counted and was then calculated as the number of parasites per microliter by assuming a leukocyte count of 7,000/μl. The initial thick film was considered negative if no parasites were seen after 500 leukocytes were counted.

DNA extraction. The DNA template for the nested PCR and LAMP was prepared as described previously (20). Twenty-five to 50 μl of human blood was blotted as a single spot and dried on filter paper. A single blood spot from each filter paper was excised and then incubated 4 h at room temperature and/or overnight at 4°C in 1 ml of 0.5% saponin in phosphate-buffered saline (PBS). The filter paper was washed for 30 min in PBS at 4°C and transferred into new tubes containing 200 μl of 5% Chelex-100 (Bio-Rad, Hercules, CA), and the tubes were vortexed for 30 s. The mixture was incubated at 56°C for 15 min, vortexed for 30 s, heated at 100°C for 15 min to elute the DNA, vortexed, and centrifuged

TABLE 1. Primer sets used for amplification of 18S rRNA genes in LAMP

Species	Primer	Sequence (5′→3′)
Plasmodium genus	F3	GTATCAATCGAGTTTCTGACC
	B3c	CTTGTCACTACCTCTCTTCT
	FIP (F1c-F2)	TCGAACTCTAATTCCCCGTTACCTATCAGCTTTTGATGTTAGGGT
	BIP (B1-B2c)	CGGAGAGGGAGCCTGAGAAATAGAATTGGGTAATTTACGCG
	LPF	CGTCATAGCCATGTTAGGCC
	LPB	AGCTACCACATCTAAGGAAGGCAG
P. falciparum	F3	TGTAATTGGAATGATAGGAATTTA
	B3c	GAAAACCTTATTTTGAACAAAGC
	FIP (F1c-F2)	AGCTGGAATTACCGCGGCTG GGTTCCTAGAGAAACAATTGG
	BIP (B1-B2c)	TGTTGCAGTTAAAACGTTCGTAGCCCAAACCAGTTTAAATGAAAC
	LPF	GCACCAGACTTGCCCT
	LPB	TTGAATATTAAAGAA
P. vivax	F3	GGAATGATGGGAATTTAAAACCT
	B3c	ACGAAGTATCAGTTATGTGGAT
	FIP (F1c-F2)	CTATTGGAGCTGGAATTACCGCTCCCAAAACTCAATTGGAGG
	BIP (B1-B2c)	AATTGTTGCAGTTAAAACGCTCGTAAGCTAGAAGCGTTGCT
	LPF	GCTGCTGGCACCAGACTT
	LPB	AGTTGAATTTCAAAGAATCG
P. malariae	F3	CAAGGCCAAATTTTGGTT
	B3c	CGGTTATTCTTAACGTACA
	FIP (F1c-F2)	TATTGGAGCTGGAATTACCGCGATGATGGGAATTTAAAACCT
	BIP (B1-B2c)	AATTGTTGCAGTTAAAACGCCTATGTTATAAATATACAAAGCATT
	LPF	GCCCTCCAATTGCCTTCTG
	LPB	TCGTAGTTGAATTTCAAGGAATCA
P. ovale	F3	GGAATGATGGGAATTTAAAACC
	B3c	GAATGCAAAGAACAGATACGT
	FIP (F1c-F2)	TATTGGAGCTGGAATTACCGCGTTCCCAAAATTCAATTGGAGG
	BIP (B1-B2c)	GTTGCAGTTAAAACGCTCGTAGTGTATTGTCTAAGCATCTTATAGCA
	LPF	TGCTGGCACCAGACTTGC
	LPB	TGAATTTCAAAGAATCAA

(10,000 × *g* for 5 min). The supernatant was either used immediately in the reaction or stored in aliquots at −20°C.

Nested PCR. For nested PCR, the species-specific nucleotide sequences of the 18S rRNA genes of *P. falciparum*, *P. vivax*, *P. malariae*, and *P. ovale* were amplified as described previously (7), with slight modifications. In the first PCR, 2 μl of template DNA (corresponding to approximately 0.25 to 0.5 μl of blood) was added to a 20-μl PCR mixture that consisted of 0.4 μM each universal primer (P1 forward primer [5′-ACGATCAGATACCGTCGTAATCTT-3′] and P2 reverse primer [5′-GAACCCAAAGACTTTGATTTCTCAT-3′]), 200 μM each deoxynucleoside triphosphate, 25 mM $MgCl_2$, 1× PCR Gold Buffer II (50 mM KCl, 15 mM Tris-HCl, pH 8.0), and 0.25 U AmpliTaq Gold DNA polymerase. The DNA amplification was carried out under the following conditions: 94°C for 10 min and then 35 cycles at 92°C for 30 s, 60°C for 1.5 min, and 72°C for 1 min, followed by a final extension at 72°C for 5 min. The first PCR product was diluted 20-fold in sterile water. One microliter of this solution was used in the second amplification. The second PCR was performed at 94°C for 10 min and then 20 cycles at 92°C for 30 s, 60°C for 1.5 min, 72°C for 1 min, followed by a final extension at 72°C for 5 min with the P1 forward primer in combination with each species-specific reverse primer (*P. falciparum*, 5′-CAATCTAAAAGTCAC CTCGAAAGATG-3′; *P. vivax*, 5′-CAATCTAAGAATAAACTCCGAAGAGA AA-3′; *P. malariae*, 5′-GGAAGCTATCTAAAAGAAACACTCATAT-3′; *P. ovale*, 5′-ACTGAAGGAAGCAATCTAAGAAATTT-3′). The amplified products were visualized in 2% agarose gels stained with ethidium bromide. The expected band sizes were approximately 160 bp for the first PCR product and approximately 110 bp for the second one. To prevent cross-contamination, different sets of pipettes and distinct work areas were used for DNA template preparation, PCR mixture preparation, and DNA amplification. Moreover, 1 uninfected blood sample was included for every 10 samples processed.

LAMP conditions. The LAMP primer sets for *P. falciparum* were described previously (21). The remaining *Plasmodium* genus- and species-specific LAMP primer sets were designed on the basis of the genus- and the species-specific nucleotide sequences of the 18S rRNA genes of *P. falciparum*, *P. vivax*, *P. malariae*, and *P. ovale* by use of the LAMP primer design software PrimerExplorer V3 (http://primerexplorer.jp/e/). The location and nucleotide sequence of each primer are shown in Fig. 1 and Table 1, respectively. The LAMP reaction was performed with a Loopamp DNA amplification kit (Eiken Chemical Co., Ltd., Tokyo, Japan). The reaction mixtures (25 μl) contained 1.6 to 2.4 μM each primers FIP and BIP, 0.2 μM each primers F3 and B3c, 0.8 μM each primers LPF and LPB, 2× reaction mixture (12.5 μl), Bst DNA polymerase (1 μl), and 1 to 2 μl of DNA sample (corresponding to approximately 0.125 to 0.5 μl of blood). The LAMP reaction was performed at 60°C for 100 min, and then the enzyme was inactivated at 80°C for 2 min.

Analysis of LAMP products. The LAMP reaction causes turbidity in the reaction tube proportional to the amount of amplified DNA. Therefore, the turbidity was observed with the naked eye. To confirm the sensitivity and the possibility of real-time LAMP quantification of *Plasmodium* parasites, the turbidity was also monitored with a Loopamp real-time turbidimeter (RT-160C; Eiken Chemical Co.). For further confirmation, 5 μl of the LAMP product was electrophoresed at 100 V in a 3% agarose gel, followed by staining with ethidium bromide and the use of a MassRuler DNA ladder marker (Fermentas Inc., Hanover, MD). The amplified LAMP product was validated by restriction analysis. On the basis of the restriction maps of the target sequences of each LAMP product, DdeI was selected for use for restriction analysis of genus *Plasmodium* products; HpyCH4V was selected for *P. falciparum*, *P. vivax*, and *P. malariae*; and AluI was selected for *P. ovale*. Following overnight digestion at 37°C, the digested products were analyzed by agarose gel electrophoresis.

Diagnostic threshold of LAMP results. LAMP was monitored through nephelometric analysis by recording the scattering light intensity reflected from a light source (wavelength, 660 nm) every 6 s with the help of the Loopamp real-time turbidimeter (RT-160C). The threshold value was defined as the value halfway between the mean maximum differential value (which represents a maximum velocity of the turbidity increment) − 3 standard deviations (SDs) for positive samples and the mean maximum differential value + 3 SDs for negative samples. Threshold values were as follows: for the *Plasmodium* genus, 0.0041; for *P.*

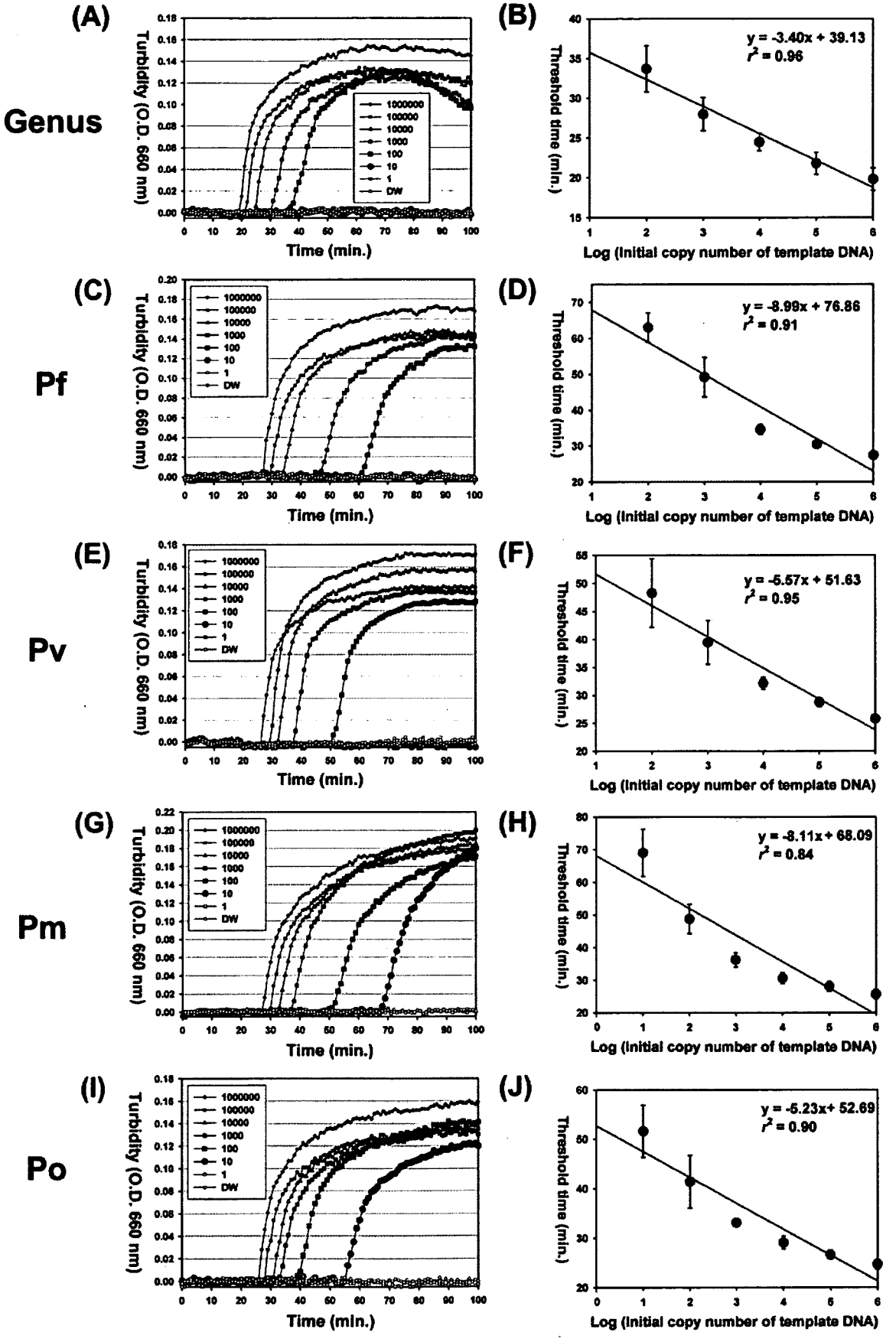

falciparum, 0.0036; for *P. vivax*, 0.0040; for *P. malariae*, 0.0043; and for *P. ovale*, 0.0045. The threshold time represented the time for the turbidity to increase to the threshold value. Most of the positive samples tested multiple times showed positivity within 1 h. Therefore, a sample with a turbidity greater than or equal to the threshold value within 1 h, as determined with the turbidimeter, was considered positive.

Positive control plasmid DNA and sequencing. For sensitivity assessment, plasmids containing the target region of the 18S rRNA gene were constructed for each species for use in the LAMP reaction. The target DNA sequence was amplified with two LAMP primers (primers F3 and B3c) by PCR with ExTaq DNA polymerase (Takara Bio Inc., Otsu, Japan) and was then cloned into the pCR2.1-TOPO TA cloning vector (Invitrogen, Carlsbad, CA), according to the manufacturer's instructions. Plasmid DNA purification was performed with a QIAprep Miniprep kit (QIAGEN, Hilden, Germany). The nucleotide sequences were determined with a BigDye Terminator sequencing kit (Applied Biosystems, Foster City, CA) by using an automated DNA sequencer (ABI PRISM 310 genetic analyzer; Applied Biosystems), according to the manufacturer's instructions. The resulting sequences were aligned by using the 18S rRNA sequences for the four species of *Plasmodium* deposited in GenBank to confirm that the target sequences were correct.

Analytical sensitivity and specificity of LAMP. To establish the minimum copy number (lower detection limit) of the target gene sequence detectable by LAMP, positive control plasmid DNAs were used. The standard curve for LAMP was constructed by using 10-fold serial dilutions of plasmid DNA (10^6 copies to 1 copy) to sterile water. For each standard, the copy number was plotted against the threshold time. The resulting plots were analyzed by linear regression, and the statistical significance of the r^2 values was analyzed by analysis of variance. Probabilities of less than 0.05 were considered statistically significant. The specificities of the genus- and the species-specific LAMP assays were evaluated with each control plasmid DNA and *P. falciparum* genomic DNA (gDNA) purified from strain NF54, *P. vivax* gDNA purified from strain Sal-I, *P. malariae* gDNA purified from strain Uganda, *P. ovale* LS type gDNA purified from a Thai isolate, *P. ovale* CDC type gDNA purified from a CDC strain, *P. knowlesi* gDNA purified from strain H, and *P. yoelii* gDNA purified from strain 17XNL.

Clinical sensitivity and specificity. The clinical sensitivity and specificity of the *Plasmodium* LAMP were calculated by using 121 whole-blood samples and microscopy as the reference standard method. Sensitivity was calculated as (number of true positives)/(number of true positives + number of false negatives), and specificity was calculated as (number of true negatives)/(number of true negatives + number of false positives).

RESULTS

Analytical sensitivity and specificity of *Plasmodium* genus- and species-specific LAMP. The sensitivity of LAMP for the genus *Plasmodium* and four species of malaria parasites, *P. falciparum*, *P. vivax*, *P. malariae*, and *P. ovale*, is shown in Fig. 2A, C, E, G, and I, respectively. An increase in the quantity of the initial template plasmid DNA shortened the threshold time, i.e., the amplification time required to exceed the threshold turbidity value. The detection limits for a positive turbidity signal were 10 copies for *P. malariae* and *P. ovale* and 100 copies for the genus *Plasmodium*, *P. falciparum*, and *P. vivax*. A plot of the threshold time versus the log of the initial template copy number showed a linear regression, with statistically significant regression coefficients: $r^2 = 0.96$ ($P = 0.004$) for the genus *Plasmodium*, $r^2 = 0.91$ ($P = 0.012$) for *P. falciparum*, $r^2 = 0.95$ ($P = 0.005$) for *P. vivax*, $r^2 = 0.84$ ($P = 0.010$) for *P. malariae*, and $r^2 = 0.90$ ($P = 0.004$) for *P. ovale* (Fig. 2B, D, F, H, and J, respectively).

The specificity of the *Plasmodium* species-specific LAMP was confirmed by using the gDNA of seven species of *Plasmodium*. Each species-specific LAMP amplified only the target species. The specificity of the amplification was further confirmed by restriction enzyme digestion of the LAMP products. As depicted in Fig. 3, the sizes of the resultant digestion products were in good agreement with the predicted sizes. The *Plasmodium* genus-specific LAMP amplified all four human malaria parasites (*P. falciparum*, *P. vivax*, *P. malariae*, and *P. ovale* LS and CDC types), the rodent malaria parasite (*P. yoelii* 17XNL), and the simian malaria parasite (*P. knowlesi*); all were detected within a 1-h reaction time (data not shown).

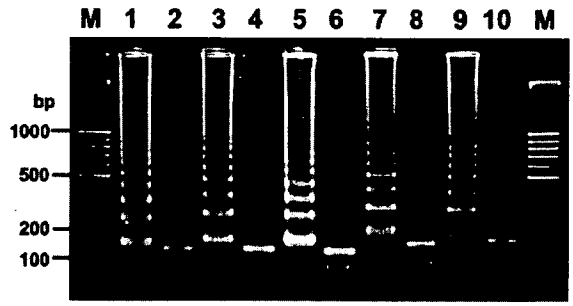

FIG. 3. Restriction analysis of *Plasmodium* genus- and species-specific LAMP products amplified from plasmid DNA containing each target 18S rRNA gene. The digestion products were run on a 3% agarose gel. Lane M, DNA ladder marker; lane 1, genus *Plasmodium* LAMP product; lane 2, DdeI digestion of genus *Plasmodium* product (123-, 44-, and 20-bp bands were expected); lane 3, *P. falciparum* LAMP product; lane 4, HpyCH4V digestion of *P. falciparum* product (130- and 79-bp bands were expected); lane 5, *P. vivax* LAMP product; lane 6, HpyCH4V digestion of *P. vivax* product (121- and 77-bp bands were expected); lane 7, *P. malariae* LAMP product; lane 8, HpyCH4V digestion of *P. malariae* product (142- and 84-bp bands were expected); lane 9, *P. ovale* LAMP product; lane 10, AluI digestion of *P. ovale* product (152- and 69-bp bands were expected).

FIG. 2. Sensitivities of *Plasmodium* genus- and species-specific real-time LAMP assays performed with serial dilutions of plasmid DNA (10^6 copies to 1 copy per reaction) containing an 18S rRNA gene. (A) Amplification with a *Plasmodium* genus-specific primer set. One representative result of four replicates is shown. Samples contained a plasmid harboring the *P. falciparum* 18S rRNA gene. (B) Plot of the mean threshold time of the *Plasmodium* genus-specific LAMP. The error bars represent the standard errors of the mean values from four replicates. The plot of the mean threshold time against the log of the input DNA fit a linear function ($r^2 = 0.96$). (C) Amplification with the *P. falciparum* species-specific primer set. One representative result of four replicates tested with the plasmid harboring the *P. falciparum* 18S rRNA gene is shown. (D) Plot of the mean threshold time of the *P. falciparum* species-specific LAMP from four replicates, which fit a linear function ($r^2 = 0.91$). (E) Amplification with a *P. vivax* species-specific primer set. One representative result of four replicates tested with plasmid harboring *P. vivax* 18S rRNA gene is shown. (F) Plot of the mean threshold time of the *P. vivax* species-specific LAMP from four replicates, which fit a linear function ($r^2 = 0.95$). (G) Amplification with a *P. malariae* species-specific primer set. One representative result of four replicates tested with a plasmid harboring the *P. malariae* 18S rRNA gene is shown. (H) Plot of the mean threshold time of the *P. malariae* species-specific LAMP from four replicates, which fit a linear function ($r^2 = 0.84$). (I) Amplification with a *P. ovale* species-specific primer set. One representative result of four replicates tested with a plasmid harboring the *P. ovale* 18S rRNA gene is shown. (J) Plot of the mean threshold time of the *P. ovale* species-specific LAMP from four replicates, which fit a linear function ($r^2 = 0.90$). Genus, genus *Plasmodium* LAMP; Pf, *P. falciparum* LAMP; Pv, *P. vivax* LAMP; Pm, *P. malariae* LAMP; Po, *P. ovale* LAMP; O.D., optical density.